FMH606 Master's Thesis 2022

Energy and Environmental Technology (EET)

Analysing Biocarbon from Pyrolysis in Anaerobic Digestion

Nasim Mohajeri Nav

Faculty of Technology, Natural sciences and Maritime Sciences

Campus Porsgrunn

Course: FMH606 Master's Thesis, 2022

Title: Analysing Biocarbon from Pyrolysis in Anaerobic Digestion

Number of pages: 65

Keywords: Anaerobic Digestion, Biochar, Activated Carbon, Conductivity, Biogas, Methane, Electron Transfer

Student:	Nasim Mohajeri Nav
Supervisor:	Wenche Hennie Bergland and Nabin Aryal
External partner:	Pål Jahre Nilsen and Gudny Øyre Flatabø in Scanship AS

Summary:

Anaerobic digestion is one of the efficient processes to manage solid waste. With this technology, waste converts to energy by producing biogas with high content of methane. Methane is an alternative to fossil fuels, which reduces greenhouse gas emissions. Therefore, increasing the biogas and methane production efficiency is important. Adding carbon conductive materials to anaerobic digestion can lead to more methane production by stimulating the direct electron transfer to methane-producing bacteria. In this master's thesis project, biochar and activated carbon were used as conductive biocarbon. The biochar was derived at Lindum AS in collaboration with Scanship AS and activated carbon is commercially available. To analyse the biocarbon effect, a pressurised biochemical methane potential (BMP) test was set up in serum bottles under mesophilic conditions. Then the pressure of the collected gas inside the bottle was measured regularly, to obtain the gas volume. Also, the effect of biofilm formation on the surface of biocarbon particles was evaluated by reusing the particles. The biocarbon surface was monitored by Scanning Electron Microscopy (SEM) to observe microorganisms attached, and their chemical elements on the surface were analysed by Energy Dispersive X-ray Spectroscopy (EDX).

The two different biocarbon acted differently in the digestion process. Activated carbon could improve biogas production by 3.5%, while biochar decreased it, but biochar increased the methane percentage to more than 85%. pH increasing to more than 8.5 in addition to biochar, was one of the main inhibitors in biogas production. This pH development was mainly due to the high ash content of biochar. Thus, to take advantage of this biochar and similar ones, a lower load should be added to prevent pH development by presenting a high amount of ash. Although the biochar is less conductive than activated carbon, it is expected that providing optimum pH for microorganisms, can result in more biogas and methane production.

Preface

This was carried out on the topic of <u>Analysing Biocarbon from Pyrolysis in Anaerobic Digestion</u> in the spring of 2022 to fulfil the master's program requirement of the Energy and Environmental Technology at the University of South-Eastern Norway.

I would like to express my deepest appreciation to my main supervisor, Associate Professor Wenche Hennie Bergland for her belief in my work, supporting, insightful suggestions and feedback, and managing the project.

I'm extremely grateful to my co-supervisor, Nabin Aryal for his valuable advice and experience, guidance, support, and time, despite his busy schedule.

I would also like to extend my deepest gratitude to my external partner, Gudny Øyre Flatabø from Scanship AS, for relentless support, ingenious and practical suggestions, patience, helpful advice and feedback, unwavering guidance, and time, while she was busy. This work would have been impossible without her.

Special thanks to Hildegunn Hegna Haugen for helping me in providing essential items in the lab, and Eshetu Janka Wakjera and Chidapha Deeraksa for helping me with the instruments.

I sincerely hope that this research is useful and interesting for further use in Lindum AS and Scanship AS and people who find this topic interesting.

Porsgrunn, 18.05.2022

Nasim Mohajeri Nav

Contents

1 Introduction

Solid waste management is one of the critical issues that need urgent attention to prevent pollution [1]. Globally, most of the solid waste is piled up in landfills that severely emit greenhouse gases (GHG) in the form of carbon dioxide, and methane [2]. Therefore, a proper solid waste management strategy has to be implemented. Over a few decades, most European countries including Norway have shifted from landfilling methods to treatment, recycling, and source prevention [3]. Municipal waste management strategies are moving towards creating value by extracting the resources in the form of energy such as biogas, and material to create green jobs for the people [4]. That involves novel technology development and process optimization. Some of the commercial waste management technologies are recycling plants, anaerobic digestion, and incineration or pyrolysis [5].

Pyrolysis technology is one of the efficient and environmentally friendly solutions for waste management [6]. Different organic materials such as sewage sludge, municipal solid wastes, agricultural residues, and wood waste [6][7]. This process can operate in the temperature range of 300-1200 ℃ [8][9] and produces three main products (bio-oil, biochar, and pyrolysis gas). The solid part is commonly called biochar [6]. Some types of biochar may display properties such as electrical conductivity, high surface area, and adsorption, properties that can potentially promote microbiological processes such as direct interspecies electron transfer [10][11].

Anaerobic digestion (AD) is one of the widely applied technologies to treat organic solid waste. Additionally, AD has been used to produce biogas which is a mixture of carbon dioxide (CO_2) and methane (CH_4) [12]. AD has been heavily investigated to optimize the microbial degradation processes and increase the biogas production from organic waste. That includes reactor development, operational parameter optimization, waste feed pretreatment, and substrate degradation process optimization. While degrading the organic waste, big organic molecules are hydrolyzed releasing simpler molecules and electrons [13]. During the process, electrons are transferred indirectly from one microbe to another microbe. In addition to this process, electrons might transfer directly between microbes in anaerobic digestion, however, stimulating by conductive materials or external voltage is required. some criteria must be met [14]. Stimulating direct interspecies electron transfer can improve biogas production efficiency [15].

1.1 Aim

In this project biochar and activated carbon were added to the anaerobic batch digestion process to evaluate whether conductive carbon such as activated carbon is beneficial and how biochar from pyrolysed digestate compares.

The topic was investigated by using conductive materials as additives in the anaerobic digestion process and evaluating the differences in biogas and methane production, monitoring changes in parameters such as pH, alkalinity, and volatile fatty acids, and evaluating changes in particle surfaces by scanning electron microscopy. Since smaller particles of biocarbon are more beneficial in biogas production, particle size was standardized into one particle size range [16][17].

2 Literature review

There are some treatment processes and products that are used in this project. Their principles and contributing factors to their efficiency and stabilization are explained in this chapter.

2.1 Anaerobic Digestion and the Main Parameters

Anaerobic digestion (AD) is a process that occurs in different types of reactors, in the absence of oxygen. Biological oxidation of biodegradable waste happens in this process, and microorganisms break down and digest the organic materials. As the result, biogas and digestate are produced.

Biogas mainly consists of methane and carbon dioxide. Hydrogen sulphide (H_2S) and water vapor are some of the other gases that might be included in biogas. Pure methane can be achieved by treating the biogas and using it to supply heat, and electricity and produce natural gas, which can be utilized as transportation fuels [18][19][20][21][22].

Fertilizers, livestock bedding, and material for bio-based products (such as bioplastics) are some of the usages of digestate [23].

Figure 2.1 shows the main steps of an anaerobic digestion plant process and energy production [24].

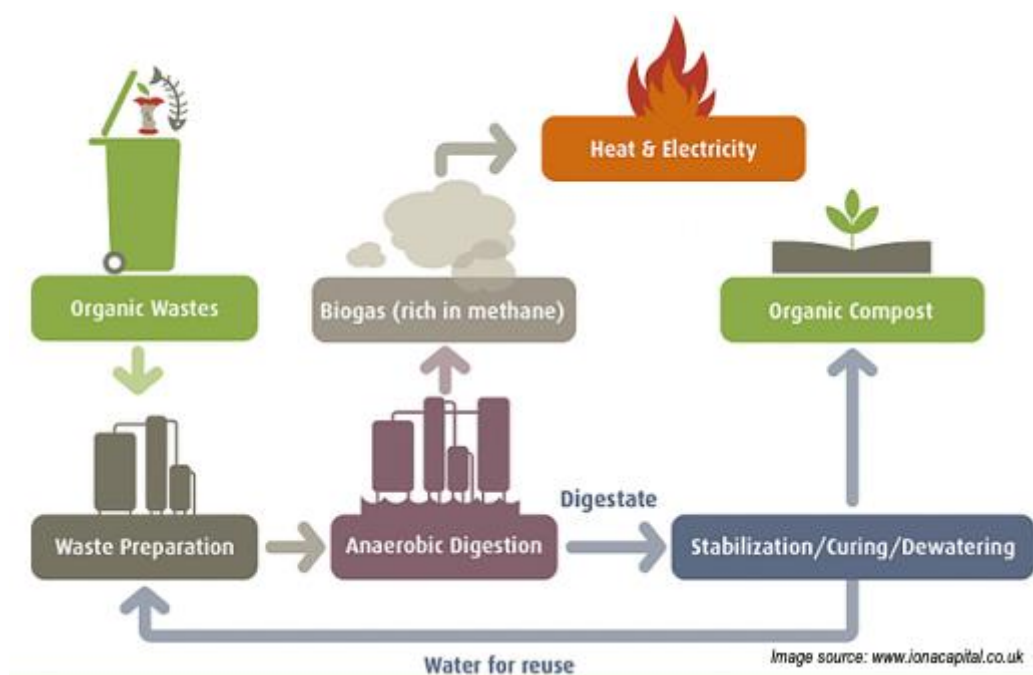Figure 2.1: Anaerobic digestion and energy production steps [24].

The four main steps in the anaerobic digestion process are Hydrolysis, Acidogenesis, Acetogenesis, and Methanogenesis [25].

The first step is hydrolysis, where complex organic polymers are broken down into simple and soluble monomers. Proteins, lipids, and carbohydrates decompose into amino acids, fatty acids, and sugar, respectively [13].

During acidogenesis, single molecules convert to ethanol and volatile fatty acids by acidogens. Carbon dioxide, hydrogen, and hydrogen sulphide are some of the minor products of this step [13][22].

The next step is Acetogenesis, where acetogenic bacteria convert the ethanol and volatile fatty acids to acetate, carbon dioxide, and hydrogen [13][22].

The fourth and last step in anaerobic digestion is methanogenesis. Methanogenesis bacteria consume acetate, carbon dioxide, and hydrogen to produce biogas, which is mainly methane and carbon dioxide [13][22][26].

Figure 2.2 illustrates the four stages of the anaerobic digestion process by microorganisms [13].
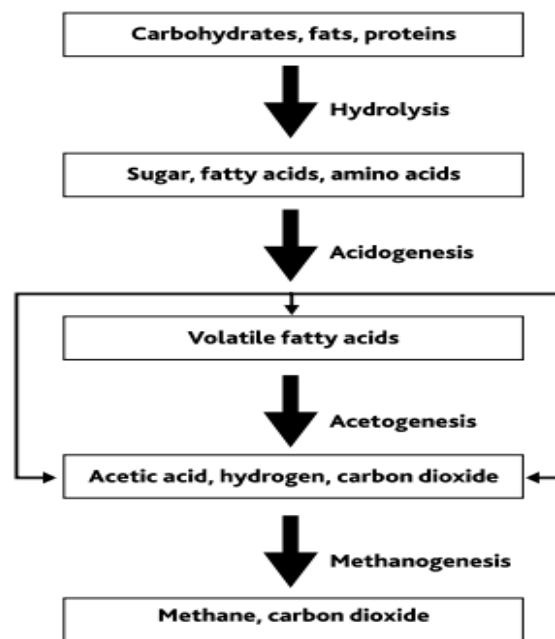

Figure 2.2: Anaerobic digestion process [13].

2.1.1 Temperature

Based on temperature, anaerobic digestion is commonly divided into psychrophilic (less than 20 °C), mesophilic (30-38°C), and thermophilic (50 to 57°C) [27][28]. Temperature strongly affects the metabolism of microorganisms, gas transfer rates, and the settling characteristics of biological sludges [28]. By reducing the digestion process temperature by around 20°C, biogas production can drop by 50%. Although in a higher temperature the digestion process and pathogen destructions occur faster and the reaction rate can increase, providing the required heat is costly, especially in cold climates. Also, thermophilic anaerobic digestion can lead to higher pH and ammonia concentration and is less stable than mesophilic digestion [28][29].

2.1.2 Alkalinity

Alkalinity consists of hydroxides, calcium, magnesium, and ammonium, sodium, potassium bicarbonates that show the buffer capacity. Alkalinity is required for the digester to achieve the

optimum pH. Around 2-5 g/L of total alkalinity provides a stable anaerobic digestion process [28][30][31].

The released carbon dioxide from methanogenesis, produces bicarbonate, carbonic acid, and carbonate alkalinity. Equation (2.1) shows the equilibrium between carbon dioxide and alkalinity [31].

$$CO_2 + H_2O \leftrightarrow H_2CO_3 \leftrightarrow H^+ + HCO_3^- \leftrightarrow H^+ + CO_3^{2-} \qquad (2.1)$$
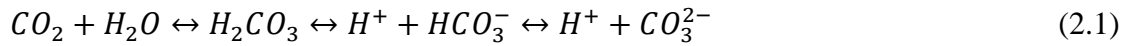
2.1.3 pH

The optimum range of pH should be provided for microorganisms' growth. At pH above 8 and less than 6.5, they cannot continue their enzymatic activity. Appendix B shows the optimum pH for different methane-forming Bacteria [32]. The production of volatile fatty acids in the digestion process decreases the pH in the beginning. After the consumption of volatile fatty acids by methanogens and the production of alkalinity, the pH increases [31].

2.1.4 Ammonium

The concentration of ammonia (NH_3) and ammonium (NH_4^+) is one of the contributing factors to the stability and efficiency of the anaerobic digestion process. It can be in the feedstock or be produced during the process by breaking down proteins. Ammonium can be helpful in bacterial growth, but its high concentration inhibits the degradation process. Inhibitor concentration of ammonium depending on some other factors can be different. For instance, in mesophilic conditions and at a pH range of 7.2 to 8, critical Total Ammonia Nitrogen (TAN) and Free Ammonia Nitrogen (FAN) can be between 2800-6000 mg/L and 337-800 mg/L, respectively [33].

2.1.5 Volatile Fatty Acids

During the acid phase of degradation of organic wastes, volatile fatty acids are produced, which are some of the main intermediates [34][28]. Measuring the concentration of volatile fatty acids is significant since they can be toxic for methane-forming bacteria by dropping the pH [35].

If there is enough alkalinity, it can neutralize the high amount of volatile fatty acids [34]. The ratio of volatile fatty acids to alkalinity is a parameter to control the stability of the anaerobic digestion process and it should be between 0.05 to 0.25 [28].

2.2 Pyrolysis

The pyrolysis process is the thermochemical treatment of the organic materials in the absence of oxygen [36]. Decomposition of materials can occur in the temperature range of 300-1200 ℃ [8][9]. Combustion does not happen in the pyrolysis process due to the absence of oxygen, however, its products are combustible [37]. Pyrolysis products are in solid (biochar), liquid (bio-oil) and gas phase (syngas) [38][36][39]. Biochar and bio-oil have lower Global Warming Potential than fossil fuels. They can reduce greenhouse gases emission by 2835 kg CO2/m3 pyrolysis oil (0.079 kg CO2/MJ) [40].

Depending on the operational conditions, there can be several types of conventional (carbonization), fast, and flash pyrolysis processes. Table 2.1 shows the values of operational parameters in various pyrolysis processes [41].

Table 2.1: Operational parameters in different types of the pyrolysis process [41].

Parameters	Conventional pyrolysis	Fast pyrolysis	Flash pyrolysis
Pyrolysis temperature (K)	550–950	850–1250	1050–1300
Heating rate (K/s)	0.1–1.0	10–200	<1000
Particle size (mm)	5–50	<1	<0.2
Solid residence time (s)	450–550	0.5–10	<0.5

Slow pyrolysis mainly produces biochar; however, fast pyrolysis produces mostly liquid and gaseous portions. The high heating rate and small particles in the feedstock of the flash pyrolysis, lead it to produce largely gaseous [41].

2.3 Biochar

Biochar can be used for various purposes, such as catalysis, soil amendment, water purification, and energy and gas storage. As catalysis, it can be utilized in syngas treatment, conversion of syngas into liquid hydrocarbons, and biodiesel production [42]. Consuming biochar as soil amendment improves the quality and health of the soil and declines greenhouse gas emissions [42][43]. Since biochar is sorbent for organic and inorganic pollutants, it can be used for soil and water treatment [44]. Furthermore, CO_2 adsorbent, the fuel source for direct carbon fuel cell (DCFC), raw material for making supercapacitors, and activated carbon are some of the other benefits of biochar [45][42].

2.4 Pressurized Biochemical Methane Potential (BMP) Test

The biochemical methane potential (BMP) test in serum bottles was developed by Owen et al. (1979) by using the Warburg apparatus. This instrument is based on the fact that variation in gas volume at constant temperature and volume can be measured by a modification of pressure [46]. In the pressurized BMP test, the pressure of the produced and collected biogas in the headspace is measured by a manometer [47].

In this method, estimating the volume of produced biogas is more accurate, but the solubility of carbon dioxide in the liquid might cause its underestimation up to 30%, which can change the pH [48][49].

2.5 Interspecies Electron Transfer

Oxidation-Reduction Reactions occur in the anaerobic digestion process to provide energy for microorganisms. In oxidation-reduction (redox) reactions the electrons exchange between the oxidizing agent and a reducing agent [28]. Acetogens convert the alcohol and organic acids to

mainly hydrogen and acetic acid. These products are electron donors and are utilized by methanogens. This process is called indirect interspecies electron transfer (IIET). Direct interspecies electron transfer (DIET) is an alternative to IIET [14]. DIET is more effective than IIET and can be improved by using conductive materials to promote and stabilize methane production in the anaerobic digestion process [11]. Figure 2.3 illustrates the electrons transfer mechanism from electron-donating bacteria to electron-accepting methanogen via conductive material [50].
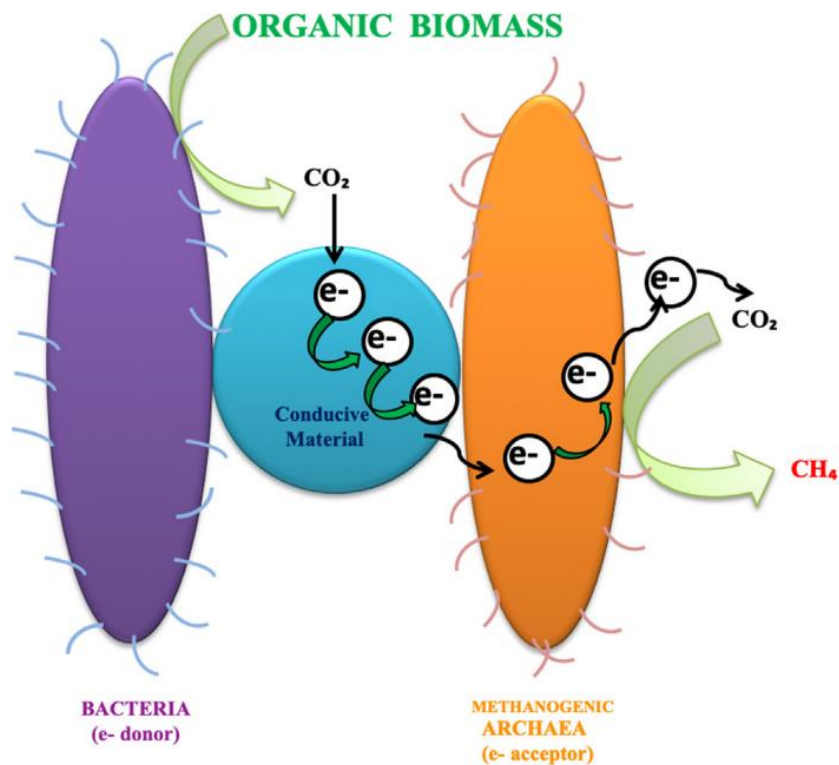

Figure 2.3: Electron transfer stimulated by conductive material [50].

Furthermore, conductive materials can act as biocarriers and improve biofilm formation [51]. Studies show that some microorganisms such as Geobacter involve in the DIET phenomenon, which conductive materials usually can generate or grow them [52][53]. In one of the researches, the presence of conductive particles could increase the abundance of Geobacter species from 6-8% to 20% [54]. Using Scanning Electron Microscope (SEM) is one of the tools to observe the colonization of bacteria on the biocarbon surface [55].

3 Materials and Methods

To evaluate the effect of biocarbon on anaerobic digestion, a biochemical methane potential experiment was set up in pressurized method. In this chapter the preparation of materials such as inoculum and biocarbon, setting up the experiment, and measurements are explained.

3.1 Inoculum Source and Preparation

The inoculum was digestate from an industrial continuously stirred-tank anaerobic digestion reactor at Lindum AS, located in Drammen. Sewage sludge and food waste are treated by a thermal hydrolysis process (THP) at 160 ℃ before digestion. The hydraulic retention time of the anaerobic digestion is about 19 days [56]. The received inoculum was sieved with a 2 mm sieve to remove coarse material and be homogenized [57][58] and kept in an incubator at 35 °C for 6 days to degas. Then it was added a mixture of vitamins, minerals, and salts to supply nutrients for microbial growth [57][59].

The volumes added to the inoculum were 1 mL/L each of vitamin mix and mineral mix and 10 mL/L of salts. Their compositions and concentrations are shown in table 3.1.

Table 3.1: Concentration of nutrient solutions ingredients.

Vitamins		**Minerals**		**Salts**	
Ingredients	Concentration (mg/L)	Ingredients	Concentration (mg/L)	Ingredients	Concentration (mg/L)
Biotin	0.02	$MnSO_4 \cdot H_2O$	0.04	NH_4Cl	100
Folic Acid	0.02	$FeSO_4 \cdot 7H_2O$	2.7	NaCl	10
Pyridoxine Hydrochloride	1	$CuSO_4 \cdot 5H_2O$	0.055	$MgCl_2 \cdot 6H_2O$	10
Riboflavin	0.05	$NiCl_2 \cdot 6H_2O$	0.1	$CaCl_2 \cdot 2H_2O$	5
Thiamine	0.05	$ZnSO_4 \cdot 7H_2O$	0.088		
Nicotinic Acid	0.05	$CoCl_2 \cdot 6H_2O$	0.05		
Pantothenic Acid	0.05	H_3BO_3	0.05		
Vitamin B12	0.001				
P-aminobenzoic Acid	0.05				
Thioctic Acid	0.05				

The inoculum was characterized by TCOD, SCOD alkalinity, total ammonium nitrogen, volatile fatty acids, total solids, and volatile solids.

3.2 Selection of Conductive Particles

The biochar was made from dewatered and dried digestate from the same source as the inoculum and was provided by Scanship AS. The dried digestate was pelletized and pyrolysed at 700 °C with a residence time of 20 minutes using the Biogreen (R) technology [60]. A similar sample of this biochar was characterized using a variety of techniques in the MSc thesis of Dzihora, Y (2021) [61]. Activated carbon was DARCO®, 20-40 mesh particle size, granular, commercially available, and supplied by Sigma-Aldrich. Characteristic data for this product was available from the producer [62].

3.2.1 Preparation of Conductive Particles

Biochar was washed with distilled water and dried overnight at 105°C in an oven. After drying, biochar was ground and sieved with 0.5 mm and 1 mm sieves. Similarly, activated carbon particles in the size range of 0.420-0.841 mm were chosen. Figures 3.1 and 3.2 exhibit the biochar particles in the original size and after sieving, respectively. Figure 3.3 exhibit the activated carbon particles.

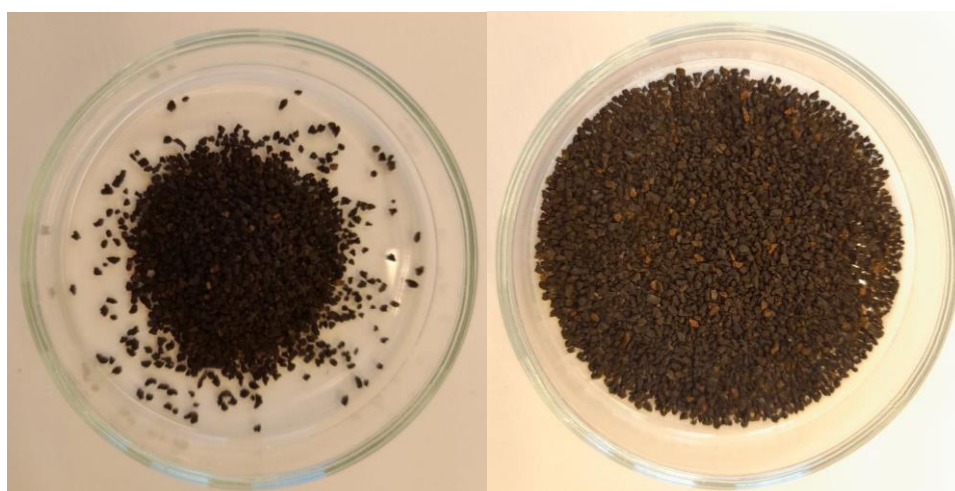Figure 3.1: Biochar particles in the original size.

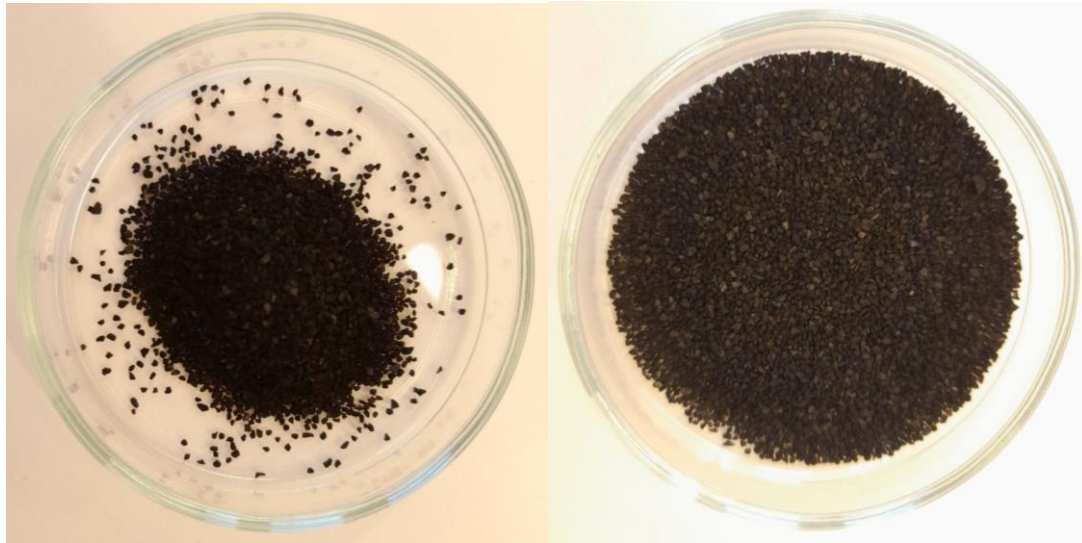Figure 3.2: Sieved biochar particles.

Figure 3.3: Activated carbon particles.

3.2.2 Characterization of Conductive Particles

The surface area of biocarbon particles was monitored by Hitachi SU3500 Scanning Electron Microscopy (SEM) before and after using them as additives in bioreactors, to evaluate forming biofilm on the particles. Figure 3.4 shows the Hitachi SU3500 Scanning Electron Microscopy. After applying in AD, the particles were frozen at -20 ℃. Freezer dryer technique was used by LabConco Freeze Dryer to remove the moisture. After that, samples were placed at SEM to observe the biofilm [63]. Energy Dispersive X-ray Spectroscopy (EDX) using Hitachi SU3500 was performed to detect the presence of the elements on the surface of the particles. Figures 3.5 and 3.6 show the biochar and activated carbon particles, respectively, after freeze-drying.

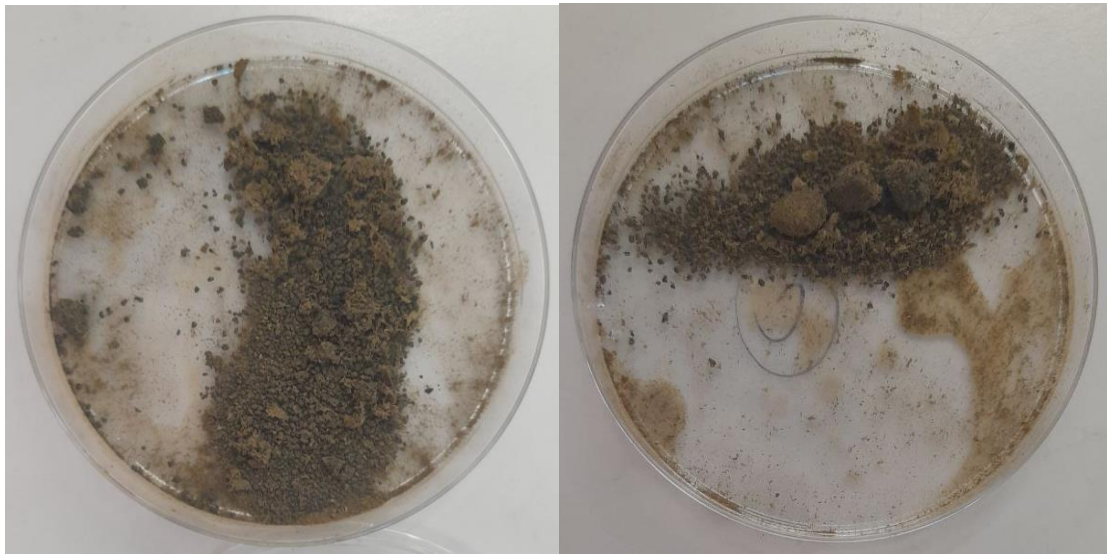Figure 3.4: Hitachi SU3500 Scanning Electron Microscopy.

Figure 3.5: Positive biochar (left) and negative control biochar (right) particles after freezing.
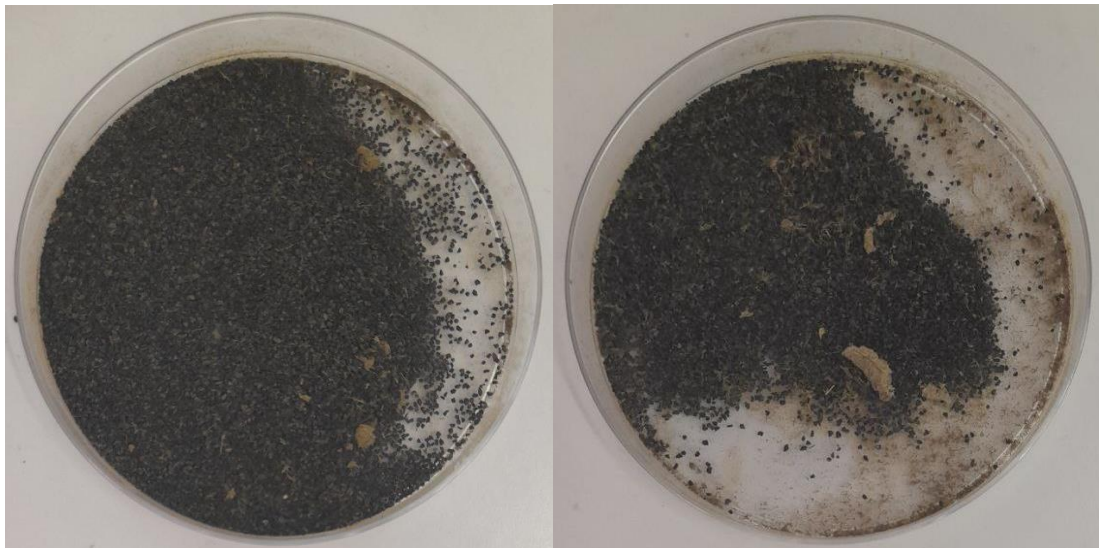

Figure 3.6: Positive activated carbon (left) and negative control activated carbon (right) particles after freezing.

3.3 Reactor Set-Up

To provide bioreactors on small scale, serum bottles were used with a total volume of 122 ml and a working space of 50 ml (41%). The headspace was 72 ml (59%), to allow for gas collection. Since the experiment was anaerobic, some nitrogen gas was flushed into the bottles before adding the mixture to minimize the air contact [64]. In the end, blue rubber stoppers and metal caps were used to avoid the air entering the bioreactors. Figure 3.7 shows one of the serum bottles after operating as a bioreactor.

Figure 3.7: Serum bottle as a bioreactor.

3.3.1 BMP Test

In this experiment, 6 samples were tested with 3 parallels. 30 g/L of biochar or activated carbon were added to the diluted inoculum. Also, 3 g pure ethanol was diluted with distilled water in a 20 ml volumetric glass and 1 ml of the diluted ethanol with a COD of 4.98 $g/L_{inoculum}$ was added as substrate in positive samples. Table 3.2 shows the composition of each sample. Negative control, negative control biochar, and negative control activated carbon are the corresponding blanks of positive control, positive biochar, and positive activated carbon, respectively.

Table 3.2: Composition of each sample in the BMP test.

Name	Number of Parallels	Prepared Inoculum (ml)	Ethanol (g/$L_{inoculum}$)	Biochar (BC) (g/$L_{inoculum}$)	Activated Carbon (g/$L_{inoculum}$)	Status
Blank	3	50	0	0	0	Negative Control
Ethanol	3	50	4.98	0	0	Positive Control
Ethanol+BC (Biochar)	3	50	4.98	30	0	Positive Biochar
BC (Biochar)	3	50	0	30	0	Negative Control Biochar
Ethanol+AC (Activated Carbon)	3	50	4.98	0	30	Positive Activated Carbon
AC (Activated Carbon)	3	50	0	0	30	Negative Control Activated Carbon

The bottles were placed on a continuously stirring board with a speed of 120 RPM and put in the incubator.

3.3.2 Reusing the Conductive Particles by the Second Feeding

26 days after setting up the BMP, the cumulatively produced biogas graph plateaued. Therefore, a mixture of vitamins, minerals, salts, and ethanol for positive samples was added to the bioreactors set up in section 3.3.1, with the same concentration as the beginning (first feeding). Before the second feeding (second batch), samples were taken from bottles to do analyses. In each sample, 1 ml was taken from two parallels and 2 ml was taken from another parallel. Besides that, for measuring the pH regularly, around 1 ml from each sample had been used in total. Thus, to adjust the volume, 2 or 3 ml of new feed mixture was added to the bottles. Then the experiment continued for another 24 days. At the end of the BMP experiment, characterizing tests such as COD, alkalinity, ammonium, volatile fatty acids, total solids, and volatile solids were done.

3.3.3 Measurements and Calculations

COD

To measure the COD, the COD Cell Test No. 1.14555 was used, which is in the range of $500 - 10000\ mg\ COD/L$. This method that corresponds to American Public Health Association 5220 is based on Oxidation with chromosulfuric acid and determines chromium (III) in Spectroquant® Prove 100 [65]. By adding the diluted sample into the kit, the total COD (TCOD) can be measured. For measuring the soluble COD (SCOD), the filtered sample should be added. The filtration was done through GxF/Glass and wwPTFE syringe filters with pore sizes of 1 and $0.45\mu l$, respectively, to remove particulate contaminations. Soluble COD is the chemical oxygen demand of soluble compounds [66]. After pipetting the samples and mixing, the reaction cells were heated in Spectroquant TR 620 at 148℃ for 2 hours. Then they were cooled for 30 minutes.

Ammonium

Ammonium Cell Test No. 114559 in the range of 4-80 mg/L with Indophenol blue method, which corresponds to American Public Health Association 4500-NH$_3$ was used to obtain Ammonium concentration [67][68]. Like the SCOD test, samples should be filtered through GxF/Glass and wwPTFE syringe filters.

Alkalinity

To measure the total alkalinity, represented as the concentration of $CaCO_3$, Acid Capacity Cell Test to pH 4.3 No. 101758 was utilized, which is in the range of 20-400 mg/L [69]. The added sample to the kit was filtered through GxF/Glass and wwPTFE syringe filters.

Spectroquant® Prove 100

The method of COD, ammonium, and alkalinity tests is photometric. After preparing the test kits, the concentration was measured by Spectroquant® Prove 100, which is with reference beam technology and wavelength range of 320-1100 nm [69].

Total Solids and Volatile Solids

30 ml of the sample was added into a crucible and kept in the 105 C oven overnight. After cooling and weighing, it was put in the furnace to burn at 550 C for 45 minutes. By knowing the weight of the crucible before and after adding the sample, after drying and burning, the percentage of total solids and volatile solids are calculated according to equations (3.1) and (3.2), respectively [70].

A: $weight\ of\ the\ empty\ crucible$

B: $weight\ of\ crucible\ and\ sample$

C: $weight\ of\ crucible\ and\ sample\ after\ drying$

D: $weight\ of\ crucible\ and\ sample\ after\ burning$

$Total\ Solids$: $((C-A)/(B-A)) * 100$ (3.1)

$Volatile\ Solids, VS/TS$: $((C-D)/(C-A)) * 100$ (3.2)

Biogas Volume

In the pressurized method, the pressure in the bottles was measured. Then the volume of biogas was obtained, using equation (3.3) [71]:

$PV = nRT \; Ideal \; gas \; law$

$\dfrac{PV}{T} = nR \; (constant) \; \rightarrow \dfrac{PV}{T_r} = \dfrac{P_a V_r}{T_a}$

$V = (P * Ta) * Vr/(Pa * Tr)$ (3.3)

$V = volume \; of \; biogas \; produced \; (mL)$

$P = pressure \; in \; bottle \; (kPa)$

$Ta = Ambient \; temperature \; (K)$

$Vr = headspace \; volume \; (mL)$

$Pa = ambient \; pressure \; (kPa)$

$Tr = temperature \; of \; bottle \; (K)$

In this experiment, ambient temperature, headspace volume, ambient pressure, and temperature of bottles were 25 ℃, 72 ml, 100 kPa, and 35 ℃, respectively.

Volatile Fatty Acids (VFA)

THERMO Scientific TRACE™ 1300 Gas Chromatograph (figure 3.8) was used to identify the different volatile fatty acids and their concentrations. VFA measurement samples were prepared by adding 150 µL formic acid to 1.35 mL of diluted and filtered samples by GxF/Glass and wwPTFE syringe filters. In this method, 3 µL is injected by an autosampler (Thermo Scientific AI 1310).

Figure 3.8: THERMO Scientific TRACE™ 1300 Gas Chromatograph.

Pressure

The pressure of produced biogas was measured daily by using Bourdon Dial Pressure Gauge 1bar, MAT1D10B15 (figure 3.9).

Figure 3.9: Bourdon Dial Pressure Gauge 1bar, MAT1D10B15.

Gas Chromatography

The concentration of methane, carbon dioxide, oxygen, and nitrogen in biogas was calculated according to equation (3.4) after obtaining the corresponding area from SRI 8610C Gas Chromatograph. In this method, the oven operates at 80 $°C$ with helium as carrier gas at 2.1 bars pressure and 20 mL/min flow rate. Operating FID (Flame Ionization Detector) temperature is 150 $°C$ with H_2 and airflow to FID at a rate of 25 mL/min and 250 mL/min respectively. Also, the response factor was calculated based on equation (3.5).

$$Gas\% = ((Corresponding\ Area/Total\ Area) * 100) * Response\ Factor \qquad (3.4)$$

The response factor of each gas is calculated by testing the standard gas, which was supplied by the Linde gas industry in Oslo, Norway, and contains 1% O_2, 1% N_2, 38% CO_2, and 60% CH_4.

$$Response\ Factor: Standard\ Area\%/ Standard\ Area \qquad (3.5)$$

The standard area% is obtained from gas chromatography and its percentage is calculated by dividing it by the total area.

Methane Yield

By knowing the average total produced biogas volume and methane percentage, and adjusting for methane produced in the corresponding blank, methane yield was calculated according to equation (3.6), based on g COD methane per g COD substrate. Equation (3.7) shows the calculation of methane concentration.

$$Methane\ yield\% = \frac{Methane\ Concentration\ (\frac{g\ COD}{L})}{Substrate\ (\frac{g\ COD}{L})} * 100 \qquad (3.6)$$

$$Methane\ concentration = biogas\ volume * methane\ percentage * COD\ of\ methane \qquad (3.7)$$

pH

Before setting up the experiment, the pH of biochar was measured. For measuring the pH, sieved biochar (0.5-1 mm) and distilled water were mixed with a ratio of 1:20 and stirred on a stirring board for 1 hour at the speed of 100 RPM [72]. In the sequence, it settled for half an hour, and then pH was measured by pH meter WTW inoLab 7110 (figure 3.10), calibrated by buffer 7.00 and 9.00.

After setting up the experiment, pH in the bioreactors was measured by the Horiba pH-33 LAQUAtwin Compact pH Meter (figure 3.11).

Figure 3.10: pH meter WTW inoLab 7110.
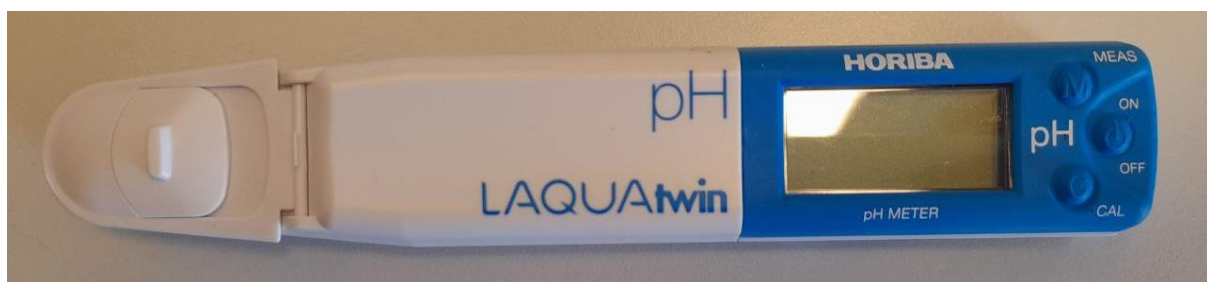
Figure 3.11: Horiba pH-33 LAQUAtwin Compact pH Meter.

4 Results

Before and after setting up the BMP test, some characterizing tests were done on the inoculum and biocarbon particles. Also, some parameters of bioreactors were measured, during the BMP test. Their results are illustrated and explained in this chapter.

4.1 Inoculum Analysis

Table 4.1 shows the results of characterizing tests on the prepared inoculum, which was added to the serum bottles.

Table 4.1: Concentration of TCOD, SCOD, ammonium, alkalinity, Total Solids (TS), Volatile Solids (VS), ash, and VFA of the prepared inoculum.

TCOD (g/L)	SCOD (g/L)	Ammonium (g/L)	Alkalinity (g/L)	TS (g/L)	VS (g/L)	VS/TS	Ash	VFA (Propionic Acid) (g/L)
24.3	4.6	2.6	8.6	25.0	14.2	60%	40%	0.09

4.2 Characteristic of Particles

The biochar used in the BMP test was characterised by SEM to monitor the surface area and EDX to identify its chemical elements on the surface.
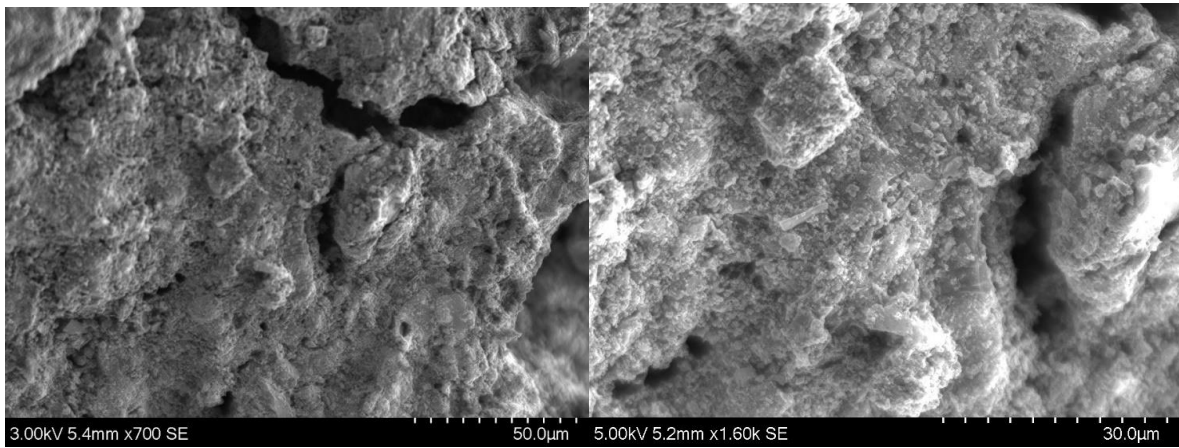
4.2.1 Surface of the Particles
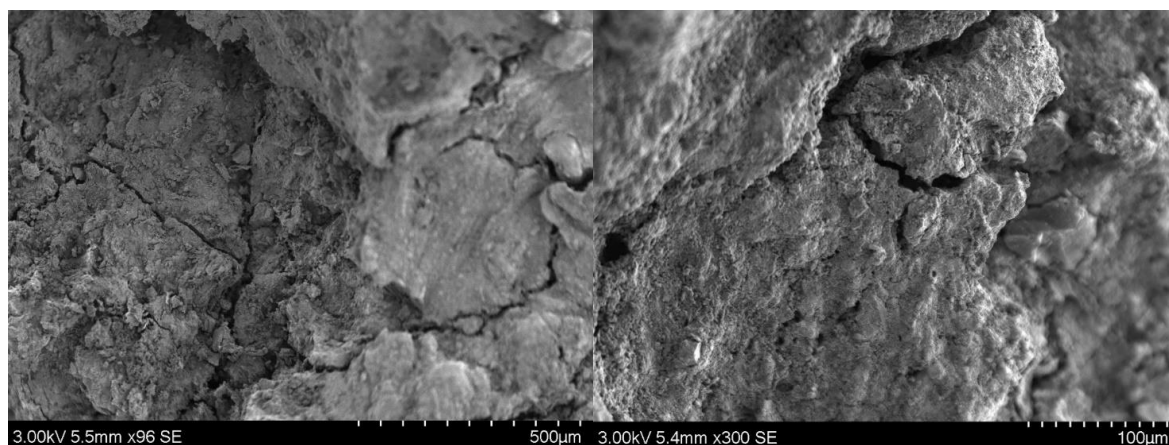
Figure 4.1: Various surfaces of the biochar particles in the original size with 500, 100, 50, and 30 micrometers dimensions and magnification of 96x, 300x, 700x, and 1600x, respectively.

Figure 4.1 shows the different surface areas of the non-sieved biochar observed by SEM in different dimensions of 500, 100, 50 and 30 micrometres and magnification of 96x, 300x, 700x and 1600x, respectively. The photos illustrate coarse surfaces on the particles.
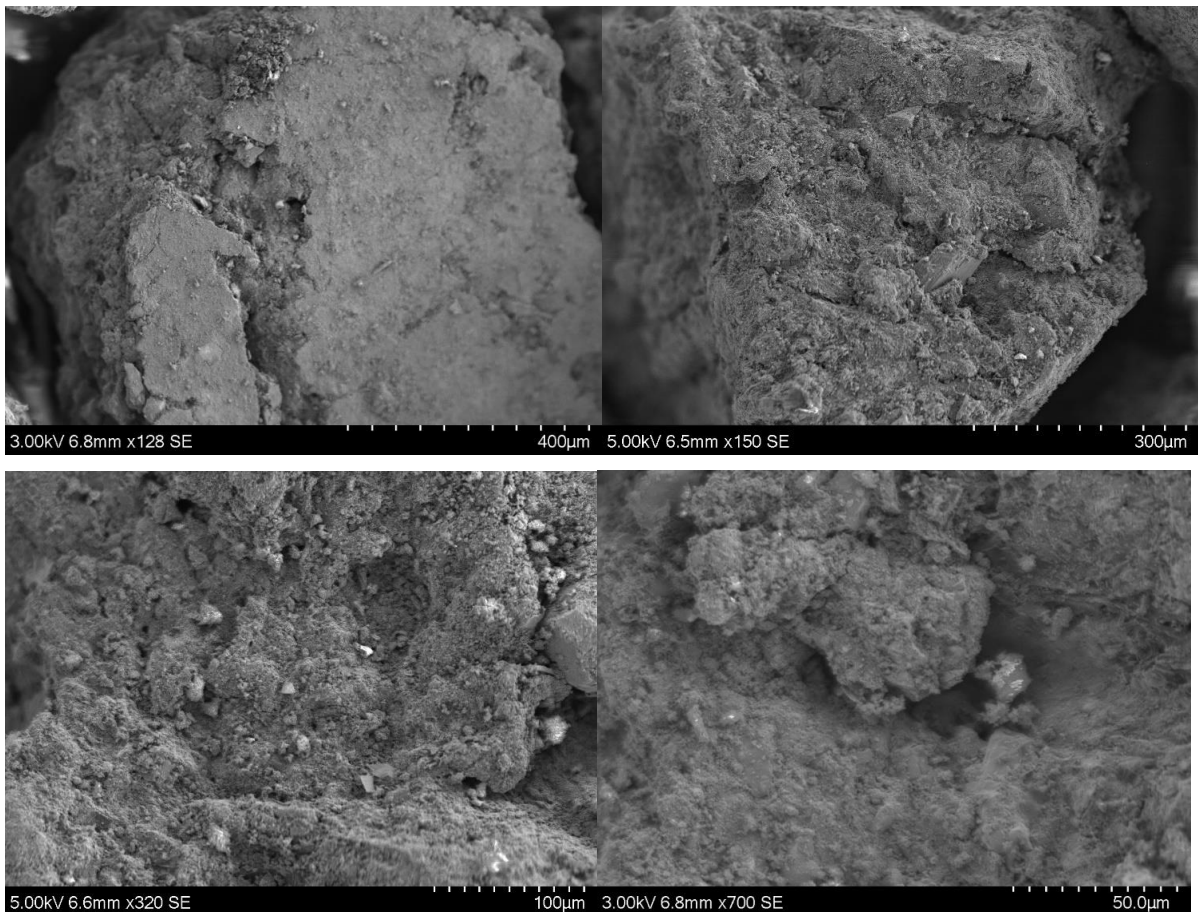

Figure 4.2: Surface of the various sieved biochar particles with a dimension of 400, 300, 100, and 50 micrometres and magnification of 128x, 150x, 320x, and 700x, respectively.

Figure 4.2 shows the surface of the sieved particles of the biochar in the dimension of 400, 300, 100, and 50 micrometres and magnification of 128x, 150x, 320x, and 700x, respectively. Similar to the main size particles, their surfaces are coarse.
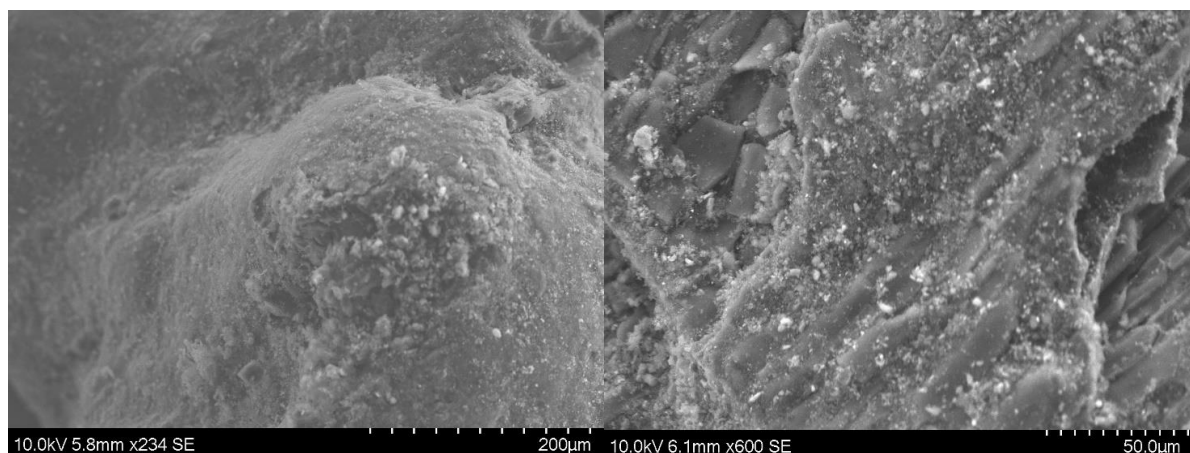

Figure 4.3: Surface of the different activated carbon particles with dimensions of 200 and 50 micrometres and magnification of 234x and 600x, respectively.
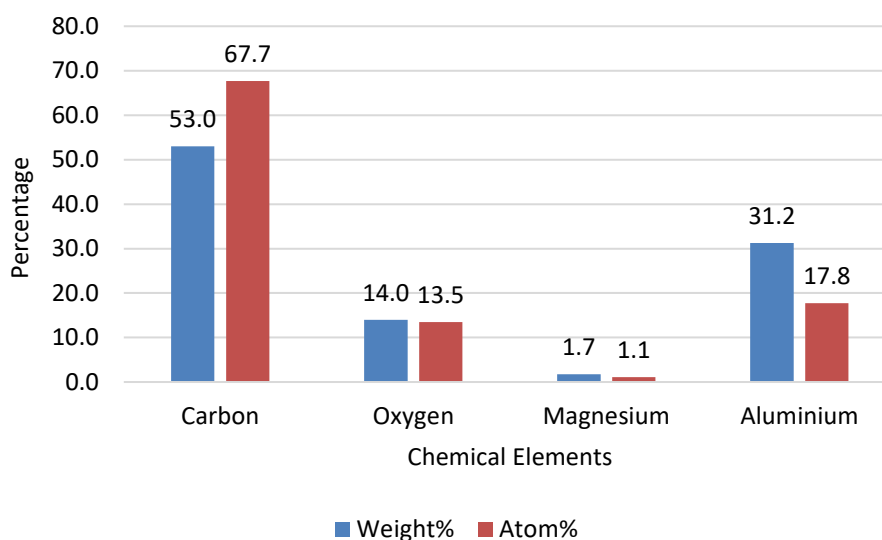
Figure 4.3 shows the surface of the activated carbon particles in the dimension of 200 and 50 micrometres and magnification of 234x and 600x, respectively.

4.2.2 Element Distribution on the Surface

Figure 4.4: Different chemical elements distributed on the surface of the original size of the biochar particle.

Figure 4.4 shows that the original size of the biochar surface mainly consists of carbon moles (67.7%). Besides carbon, it has some moles of aluminium and oxygen, 17.8% and 13.5%, respectively. The amount of magnesium atoms is very low (1.1%). This trend was also observed in mass-based, consisting of 53% carbon, 31.2% aluminium, 14% oxygen, and 1.7% magnesium.
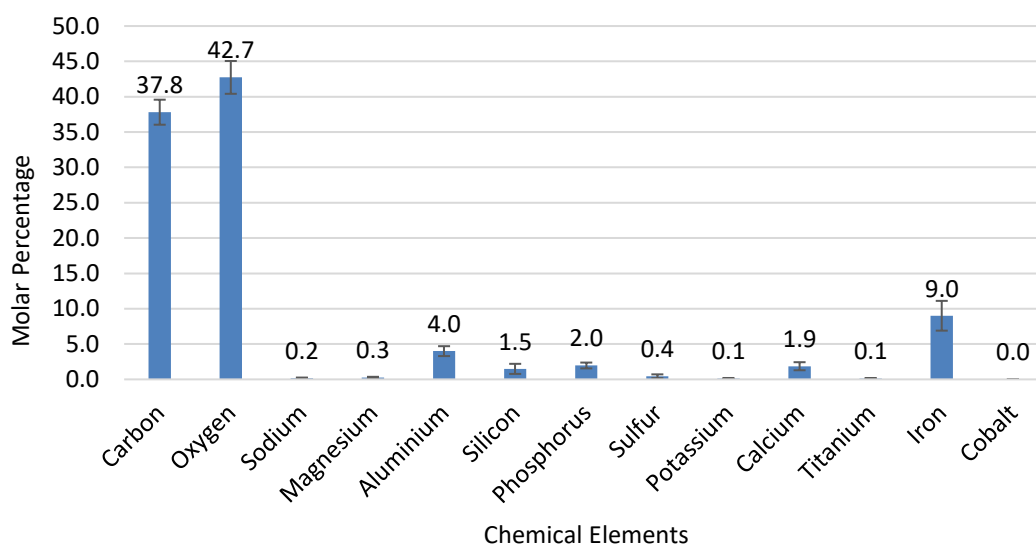
Figure 4.5: Molar percentage of different chemical elements on the surface of sieved biochar particles.

The molar percentage of chemical elements on the surface of sieved biochar is shown in figure 4.5. Sieved biochar mainly consists of oxygen and carbon, 42.7% and 37.8%, respectively. It has also 9% iron and 4% aluminium. Although there are some other chemical elements such as phosphorous, calcium, and silicon, their content is less than 2% each.
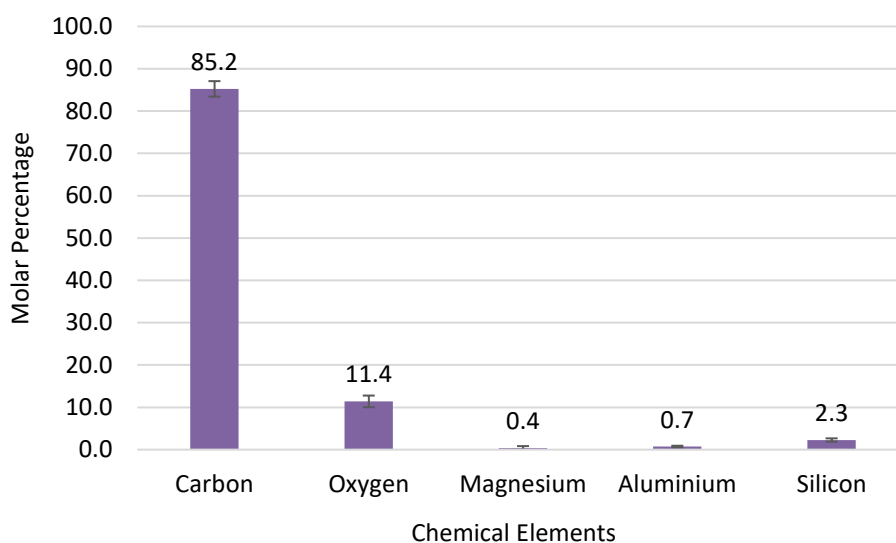

Figure 4.6: Molar percentage of different chemical elements on the surface of activated carbon particles.

Figure 4.6 shows that on the surface of the activated carbon are mainly carbon moles, for more than 85%. The rest is 11.4% oxygen. 2.3% silicon and less than 1% aluminium and magnesium moles.

4.3 Effect of Conductive Materials on Anaerobic Digestion

Anaerobic digestion parameters that were measured in the BMP test, are presented in this section.

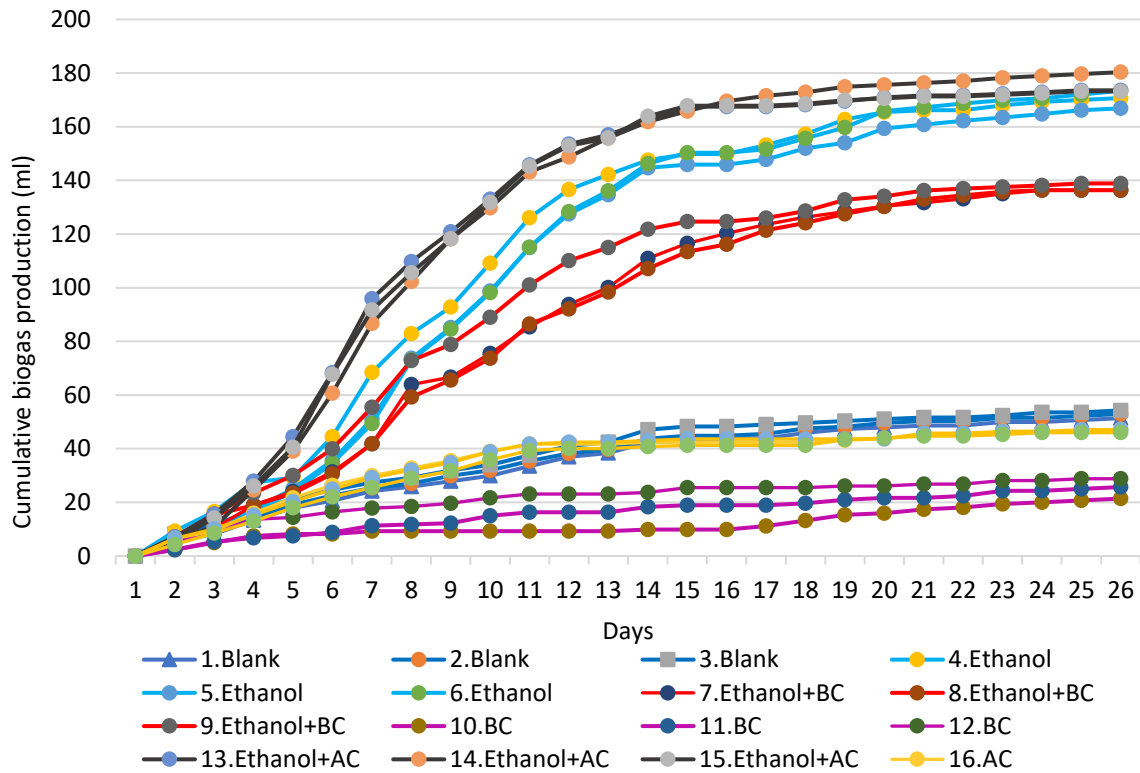## 4.3.1 Contribution to Biogas Production

Figure 4.7: Cumulative produced biogas in the first batch, over time.

Figure 4.7 illustrates cumulative biogas production during the time. Three parallels in each sample are shown in the same colour.
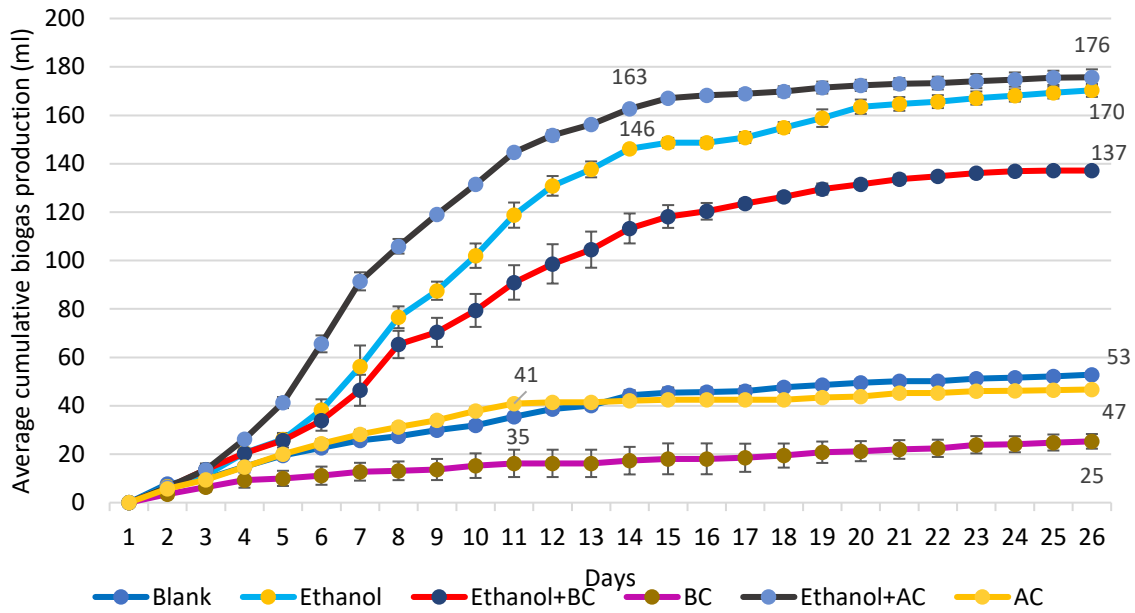
Figure 4.8: Average cumulative biogas production in the first batch, during the time and their standard deviation in bars.

Figure 4.8 shows the average volume of produced biogas by the samples. Positive activated carbon increased the biogas production compared to the control by 6 ml, $(176 - 170) * 100/170 = 3.5\%$ and reached the highest volume of biogas (176 ml). This improvement was higher in the first two weeks, which was 17 ml ((163-146)*100/146=11.6%). Also, it reduced the lag phase by 3 days. Although negative control activated carbon decreased it for 6 ml ((53-47)*100/47= 12.85%). It affected positively in the first two weeks and increased it for 6 ml ((41-35)*100/35)=17%) up to the end of day 11.

On the other hand, positive biochar and negative control biochar decreased the biogas production for 33 ml ((170-137)*100/137)=19.4%), and 28 ml ((53-25)*100/53)=52.8%), respectively. The addition of biochar led to the lowest biogas production and no significant change in the lag phase.

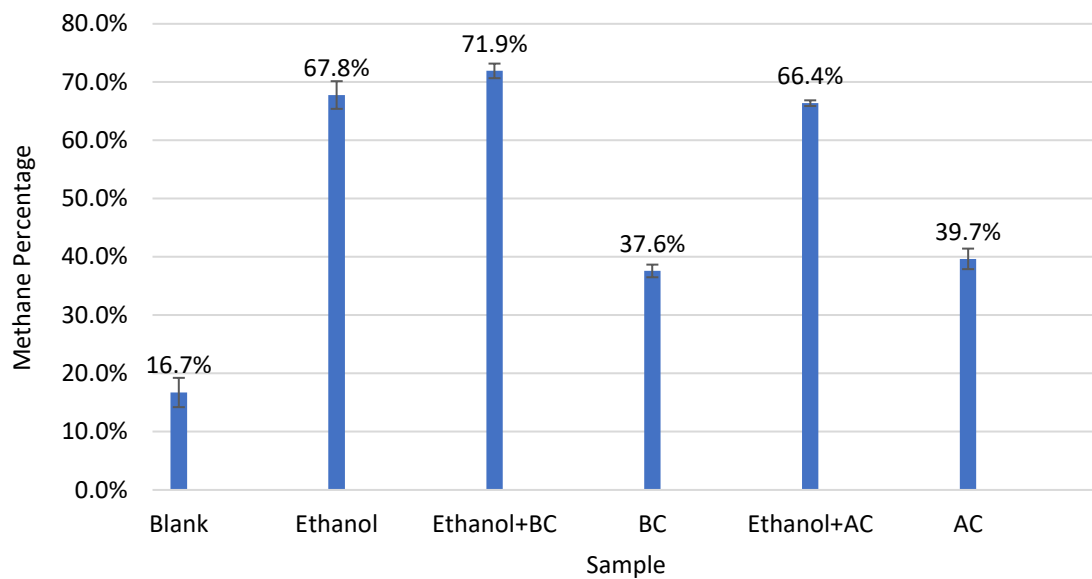## 4.3.2 Contribution to Methane Production

Figure 4.9: Average methane percentage in the first batch and the error bars.

Figure 4.9 illustrates that in positive samples, methane percentage was higher, in comparison with the negative controls. Also, biocarbon improved the methane percentage. Positive biochar improved it by 4.1% and reached the highest methane percentage (71.9%). Positive activated carbon reduced the methane percentage slightly by 1.4% (to 66.4%).

In negative control samples, both biocarbon improved the methane percentage from 17% to below 40%.
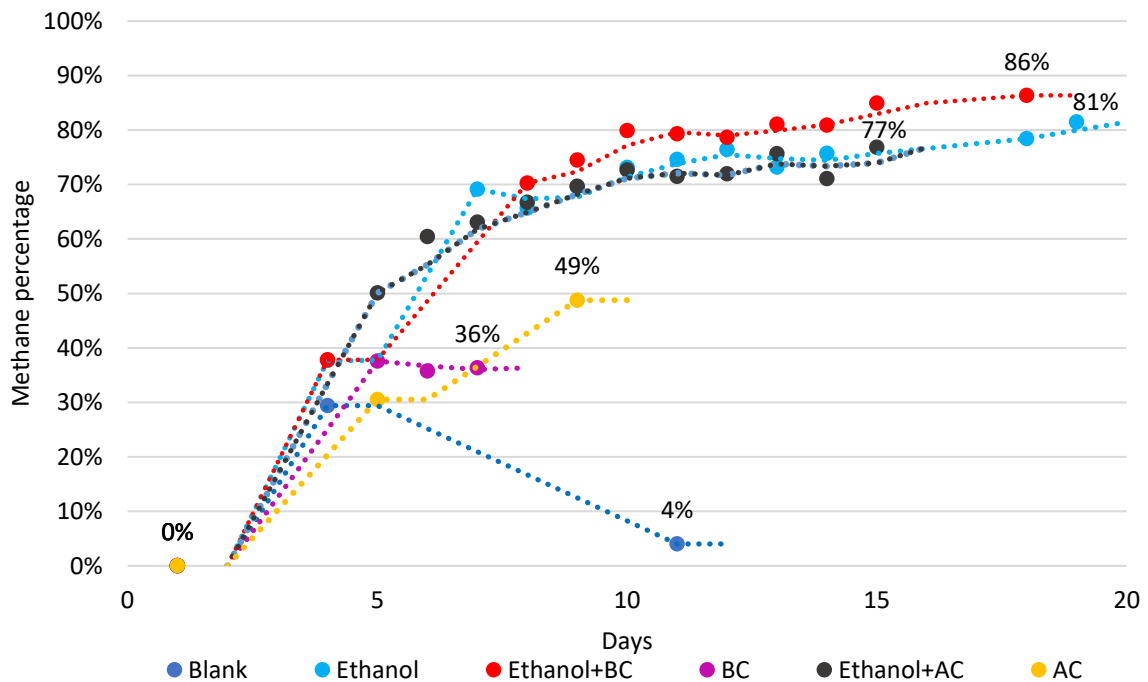

Figure 4.10: Methane percentage during the time in the first batch.

Figure 4.10 displays the variation of methane percentage in different samples. The methane percentage of positive samples raised rapidly in the first week and reached around 70%. Then, positive biochar exceeded and reached the highest percentage (86%), while positive control and positive activated carbon grew up to 81% and 77%, respectively.

In negative control samples, the methane percentage grew sharply in the first 5 days, from 0 to between 30% and 40%. Then, activated carbon increased it constantly to 49%. However, the biochar and control sample reduced it from 38 to 36 and 30 to 4%.
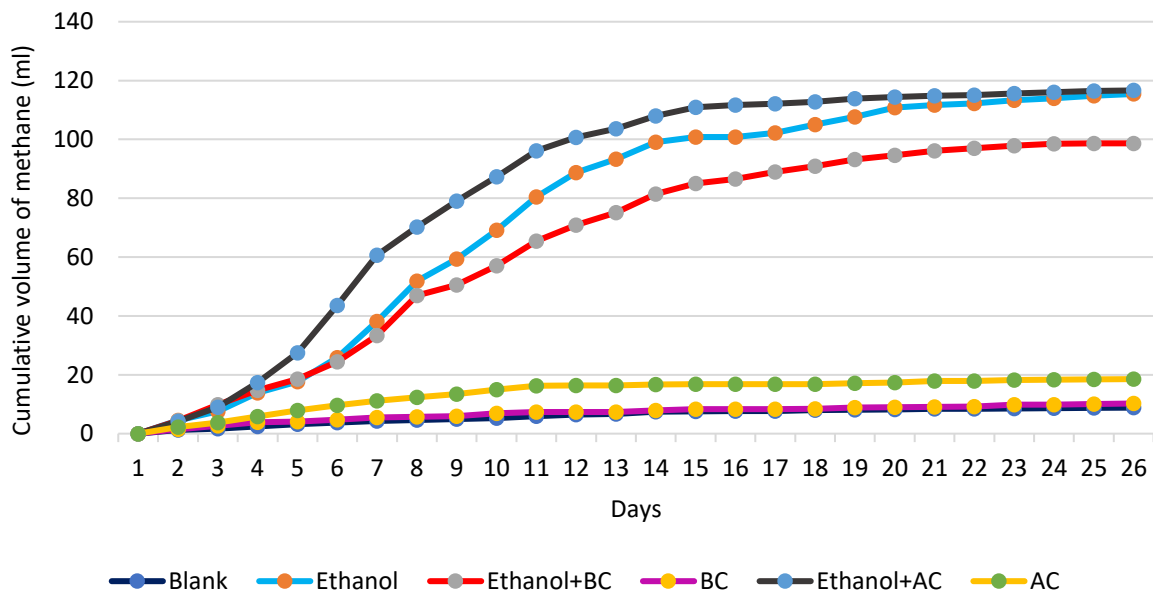

Figure 4.11: Average cumulative methane production during the time in the first batch.
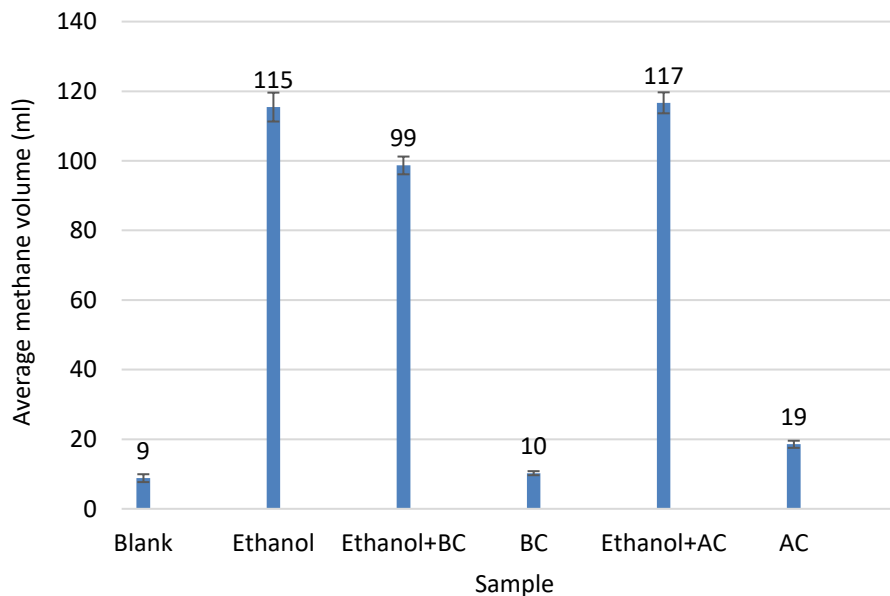

Figure 4.12: Average methane production and their standard deviation in bars in the first batch.

Applying the methane percentage to biogas production, resulted in figures 4.11 and 4.12. Positive activated carbon and positive control had the highest methane volume (117 ml and 115 ml, respectively). Although activated carbon did not improve it significantly at the end of the first batch, it increased the methane production by 11 ml ((112-101)*100/101=10.95%) after 16 days. On the opposite, positive biochar reduced it by 16 ml ((115-99)*100/115=13.9%).

Methane production trend and volume in negative control and negative control biochar were similar. They produced around 10 ml at the end. However, negative control activated carbon raised the produced methane by 19 ml.
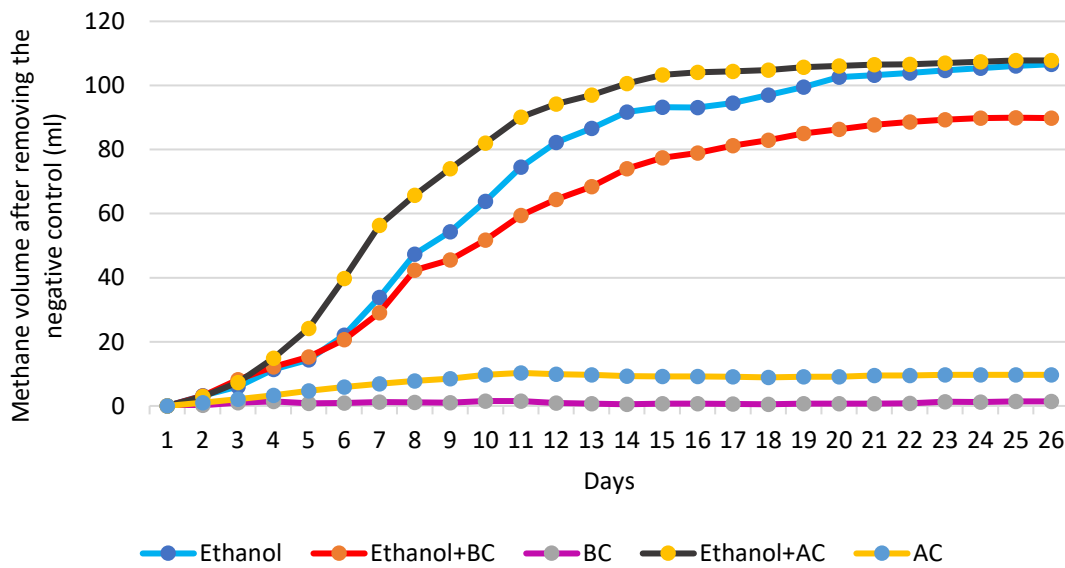

Figure 4.13: Average methane production after removing the effect of the negative control sample, over the time in the first batch.
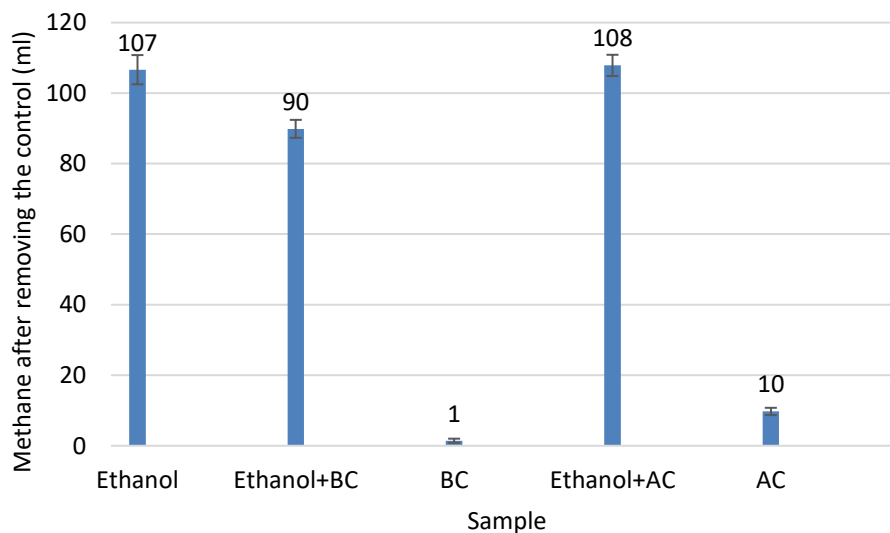

Figure 4.14: Average methane production after removing the effect of the negative control sample in the first batch and their error bars.

Figures 4.13 and 4.14 illustrate the methane volume after removing the effect of the inoculum. Positive activated carbon could increase the methane volume for only 1 ml ((108-107)*100/107=0.9%) and positive biochar decreased it for 17 ml ((107-90)*100/90=18.9%).

Negative control biochar had the lowest methane production (1 ml), but negative control activated carbon was more effective than control biochar, by producing 10 ml of methane.
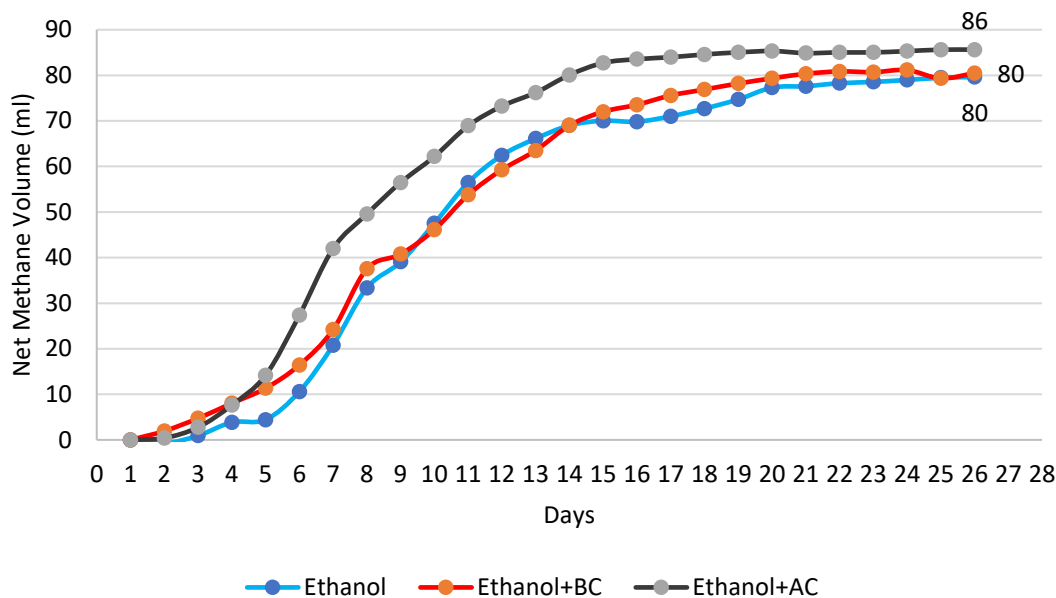
4.3.3 Methane Yield Calculation

Figure 4.15: Cumulative net methane production (volume of methane after removing the effect of corresponding blanks) in the first batch.
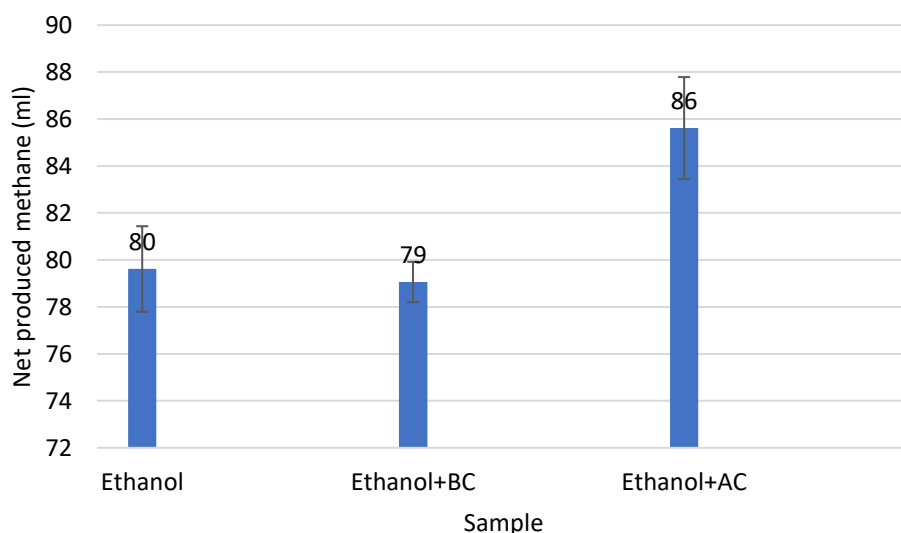

Figure 4.16: Net methane production (volume of methane after removing the effect of corresponding blanks) in the first batch and their error bars.

From figures 4.15 and 4.16 it is evident that activated carbon was more beneficial to ethanol by producing 86 ml methane. On the contrary, biochar did not modify it significantly. Although according to figure 4.15, positive biochar exceeded positive control on some of the days, both positive biochar and positive control produced around 80 ml methane at the end.
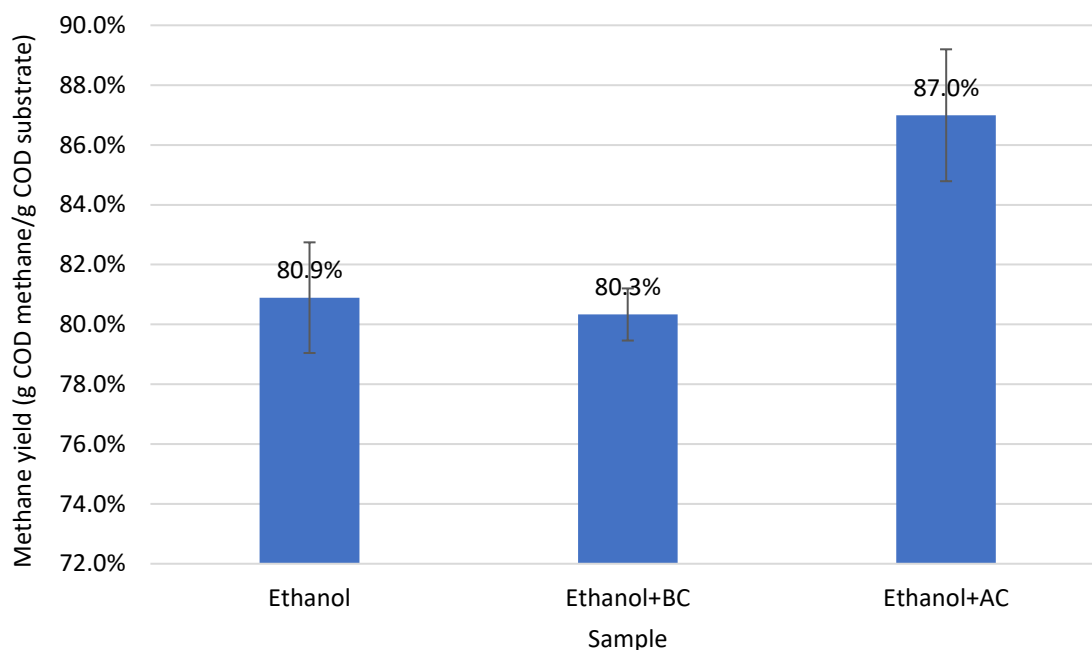

Figure 4.17: Methane yield in the first batch and their standard deviation with bars.

According to figure 4.17, in the first feeding, positive activated carbon had the most methane yield (87%) and increased it by around 6% in comparison to the positive control. On the opposite, positive biochar had the lowest methane yield (80.3%), 0.6% less than the positive control.

4.3.4 pH Variation

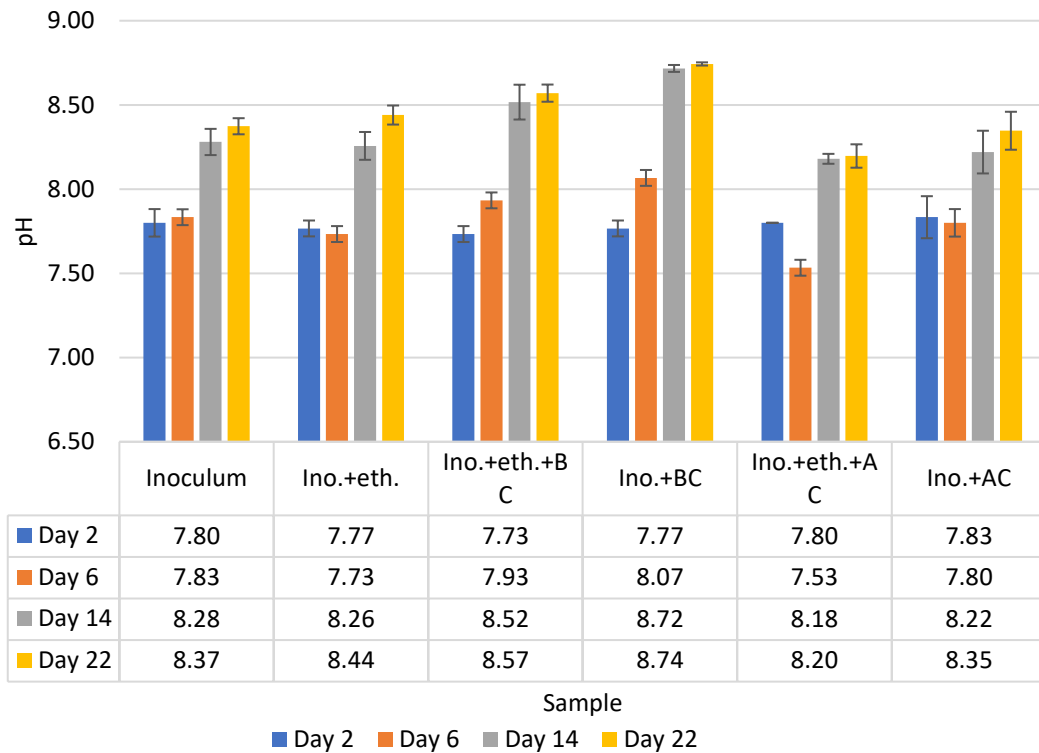|	Inoculum	Ino.+eth.	Ino.+eth.+BC	Ino.+BC	Ino.+eth.+AC	Ino.+AC
■ Day 2	7.80	7.77	7.73	7.77	7.80	7.83
■ Day 6	7.83	7.73	7.93	8.07	7.53	7.80
■ Day 14	8.28	8.26	8.52	8.72	8.18	8.22
■ Day 22	8.37	8.44	8.57	8.74	8.20	8.35

Figure 4.18: pH modification during the time and their error bars in BMP first batch.

Regarding figure 4.18, generally pH values increased over time, after a slight reduction in the first week in samples without biochar. At the beginning of the batch, all samples had almost the same pH values (around 7.8), while at the end of the first batch, positive biochar and negative control biochar had the highest pH numbers (8.57 and 8.74, respectively). A comparison of negative control and negative control activated carbon shows that the addition of activated carbon did not affect the pH. Both reached near 8.4. Only a small reduction was observed in positive activated carbon (8.2).
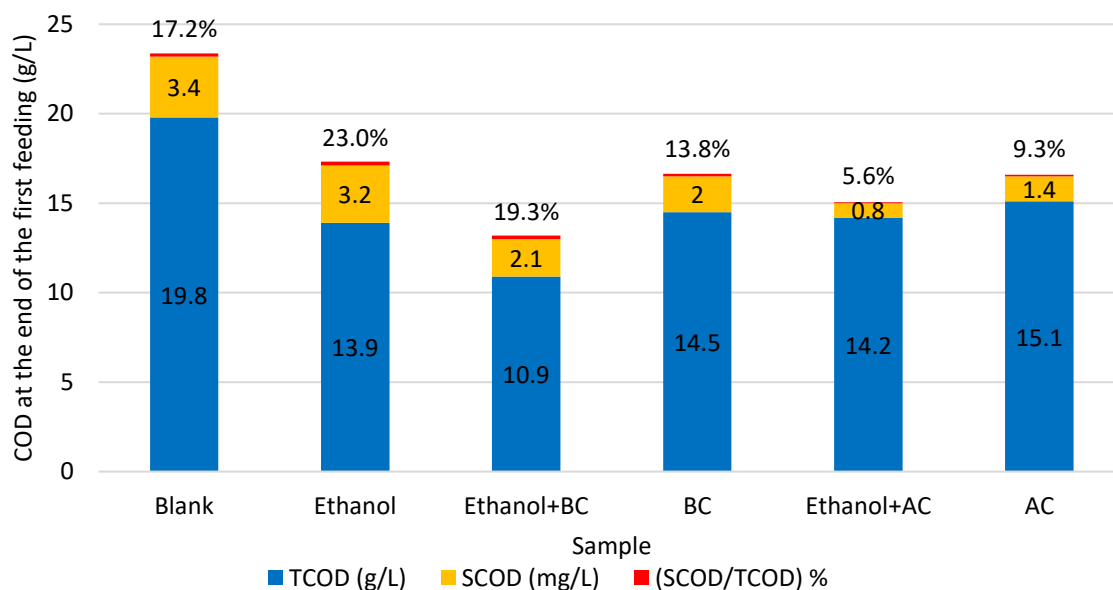
4.3.5 COD

Figure 4.19: COD concentration of the samples at the end of the first batch.

According to figure 4.19, the negative control had the highest, and positive biochar had the lowest concentration of TCOD at the end of the first batch (19.8 and 10.9 g/L, respectively). This concentration in other samples was between 14-15 g/L. Similarly, the negative control had the highest SCOD concentration (3.4 g/L) and positive activated carbon had the lowest SCOD (0.8 g/L).

Regarding the percentage of SCOD, the highest value was observed in the positive control (23%) and the lowest value observed in positive activated carbon (5.6%).
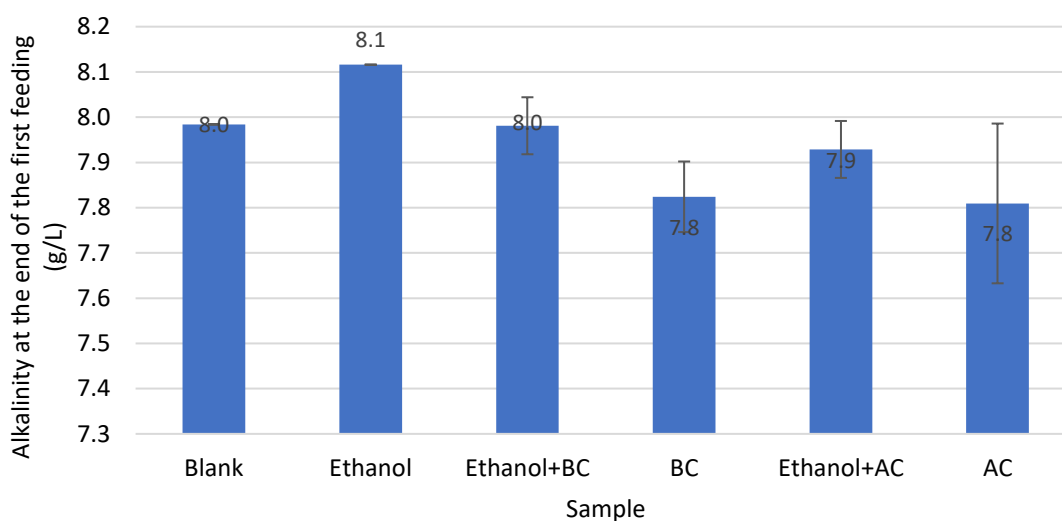
4.3.6 Alkalinity

Figure 4.20: Alkalinity concentration of the samples at the end of the first batch.

Figure 4.20 illustrates that biocarbon addition reduced the concentration of alkalinity in positive and negative control samples. This reduction was almost the same amount as biochar and activated carbon. On the other hand, the substrate increased the alkalinity in all the samples.

4.3.7 Volatile Fatty Acids (VFA)
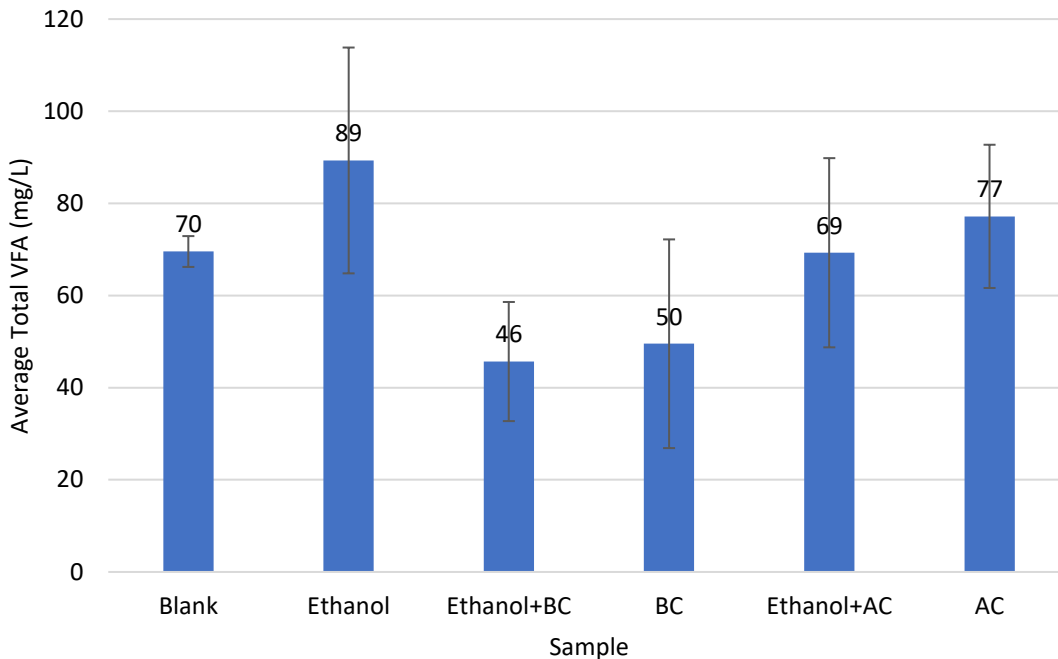
Figure 4.21: Total volatile fatty acids concentration of the samples at the end of the first batch.

According to figure 4.21, the highest concentration of VFA was observed in the positive control (89 mg/L). Positive biochar and negative control biochar that had the lowest amount of VFA, reduced it to 46 mg/L and 50 mg/L, respectively. Positive activated carbon declined it to 69 mg/L, but negative control activated carbon improved it to 77 mg/L.

4.4 Reusing the Conductive Particles by Second Feeding

The results obtained by measuring the anaerobic digestion parameters after the second feeding are presented in this section.

4.4.1 Contribution on Biogas Production

Figure 4.22: Cumulative produced biogas during the time in the second batch.
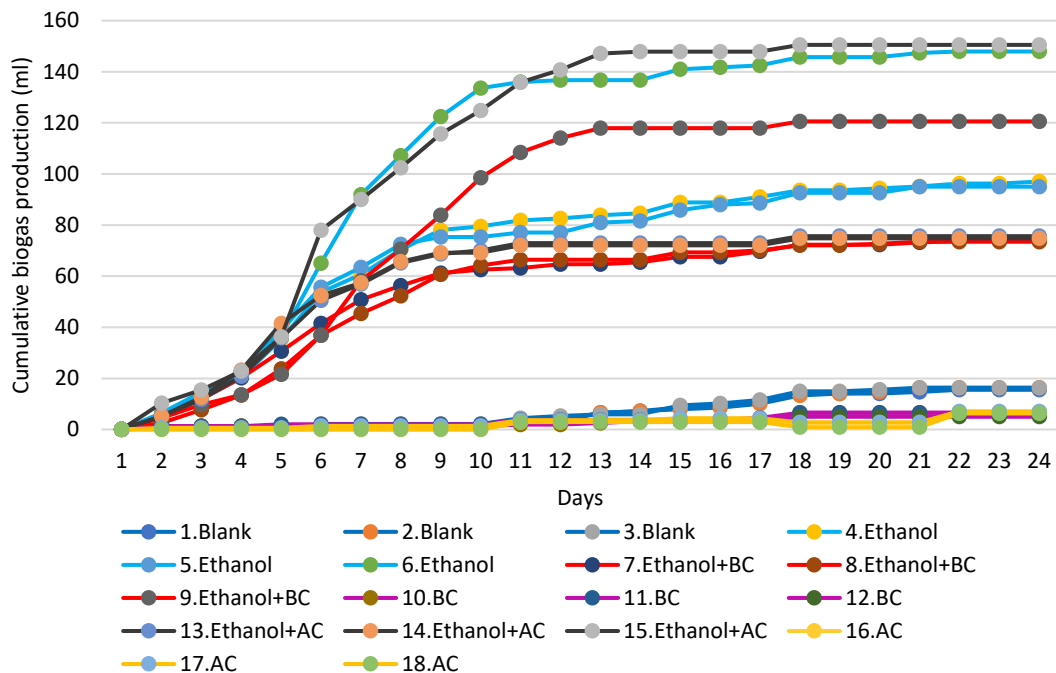
In figure 4.22 the three parallels of each sample are displayed in the same colour. In each positive sample, one parallel produced much more biogas in compare with the other two parallels.
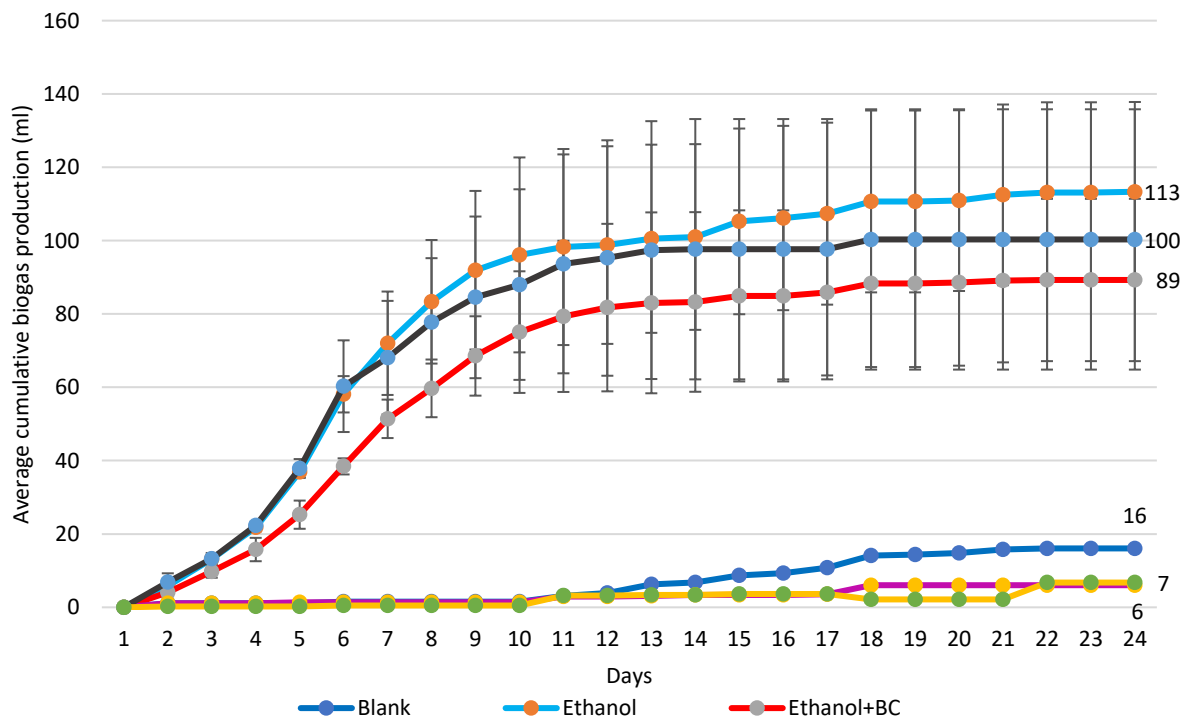
Figure 4.23: Average cumulative biogas production over time in the second batch and their error bars.
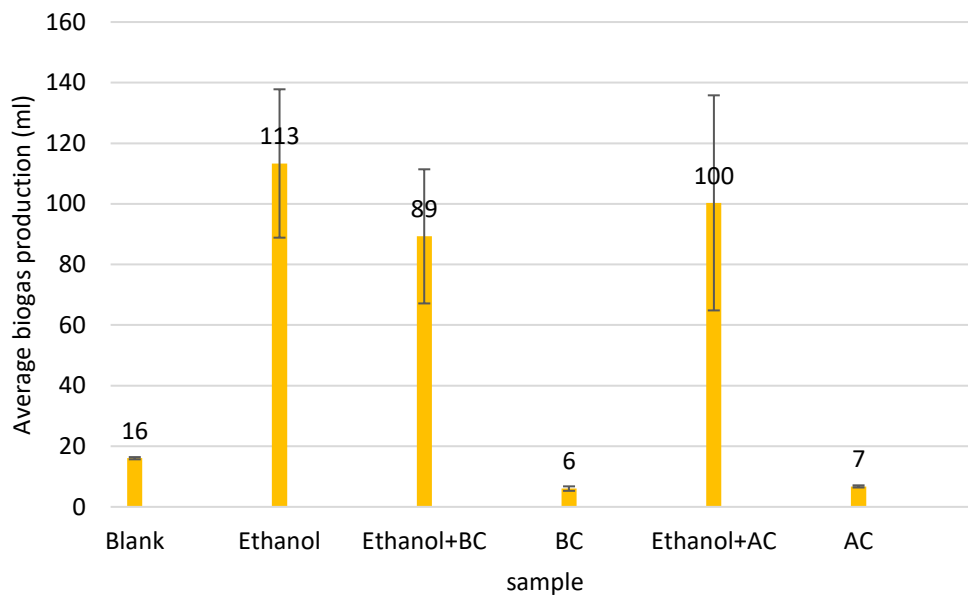
Figure 4.24: Average produced biogas in the second batch and their error bars.

Figures 4.23 and 4.24 exhibit that the positive control exceeded the positive activated carbon after 6 days and produced the most biogas at the end of the batch (113 ml). Positive activated carbon and positive biochar reduced the biogas production to 100 ml (for (113-100)*100/113=11.5%) and 89 ml ((113-89)*100/113=21.2%), respectively. Similarly, the negative control sample exceeded negative controls biocarbon after 12 days and produced more biogas (16 ml). Activated carbon and biochar declined it for around 10 ml (62.5%).

4.4.2 Contribution on Methane Production
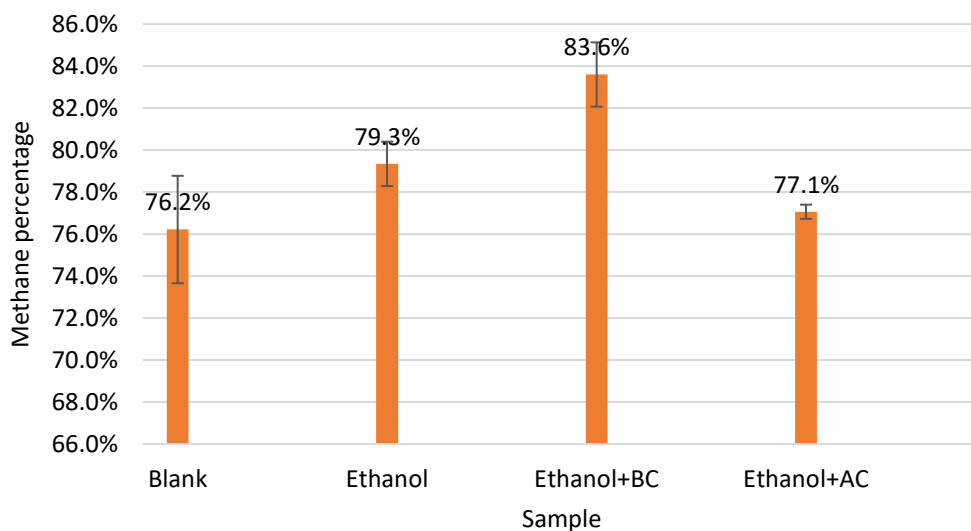
Figure 4.25: Average methane percentage in the second batch and standard deviation with bars.

Figure 4.25 that positive biochar improved methane percentage to near 84% but positive activated carbon declined it by around 2%. The negative control sample had the smallest methane percentage (76.2%).
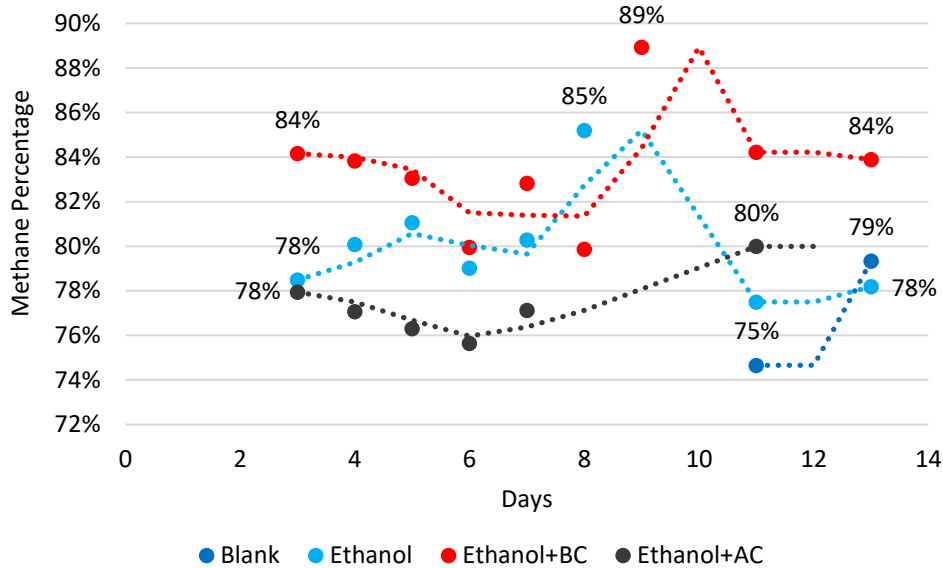
Figure 4.26: Methane percentage over the time in the second batch.

Figure 4.26 shows that the positive biochar had the highest methane percentage at the beginning and end of the second batch. It started with 84% and after gradual reductions in the first week, it increased sharply to its highest amount (89%) on day 9. Then it reduced back to 84% on day 13. Similarly, positive control started with 78% and after some fluctuations, it reduced back to 78% at the end. On day 8 it reached 85%, which was its highest amount. Methane percentage of positive activated carbon increased from 78% to 80%, after slight reductions in the first week. This number in the negative control sample improved from 75% to 79% in two days.
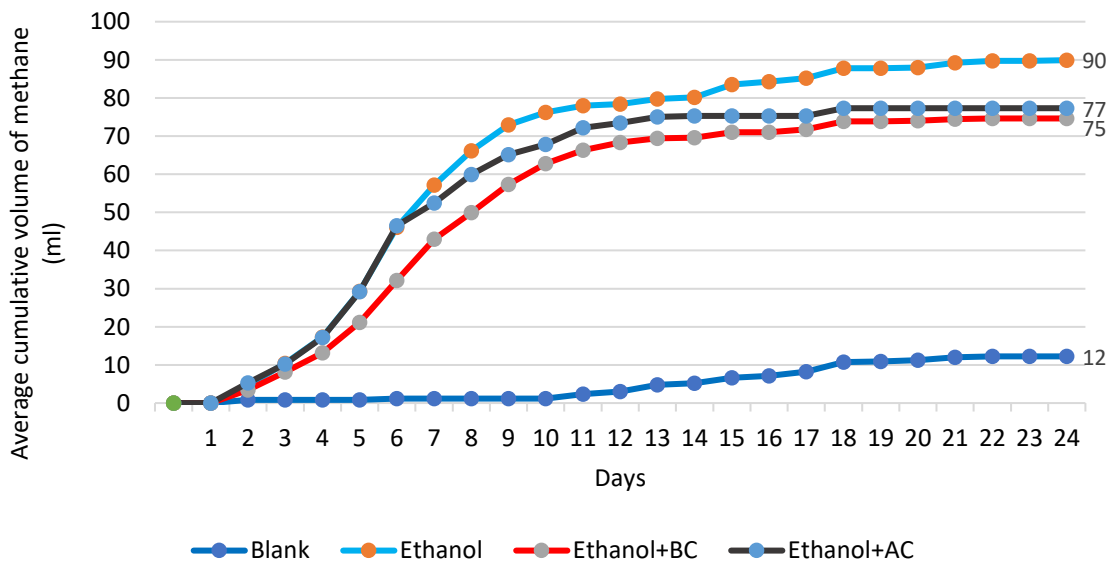
Figure 4.27: Average cumulative volume of methane, during the time in the second batch.
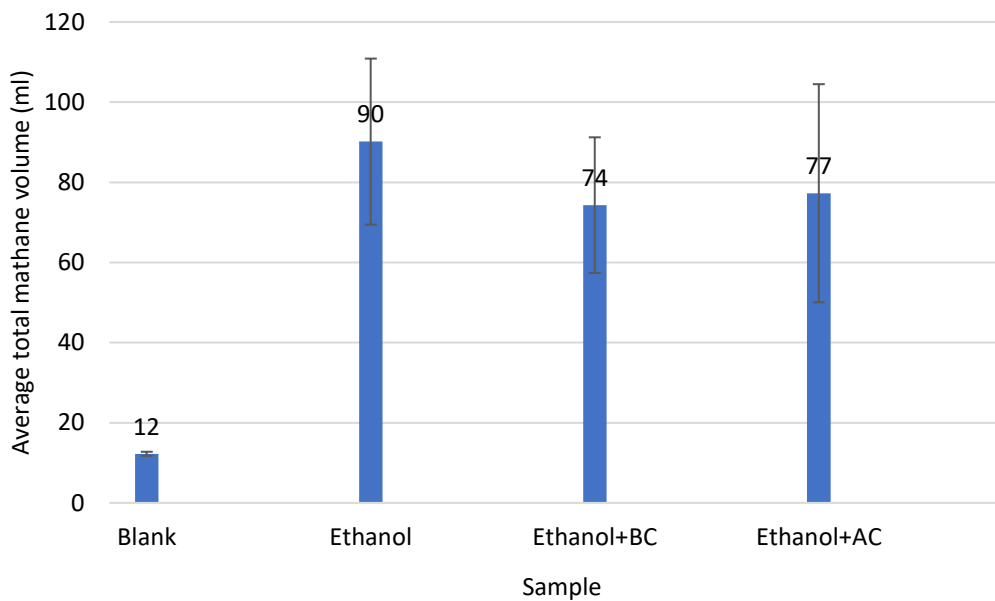
Figure 4.28: Average total volume of methane in the second batch and standard deviation with bars.

Applying methane percentage to biogas production resulted in figures 4.27 and 4.28. It can be seen that positive control had the most methane production (90 ml). Also, positive biocarbon declined methane production (16 ml and 13 ml by positive biochar and positive activated carbon, respectively). In the first two weeks, positive activated carbon produced much more methane than positive biochar, but at the end of the batch, it was higher only for 2 ml.

The lowest methane was produced by the negative control sample (12 ml).

4.4.3 Methane Yield Calculation
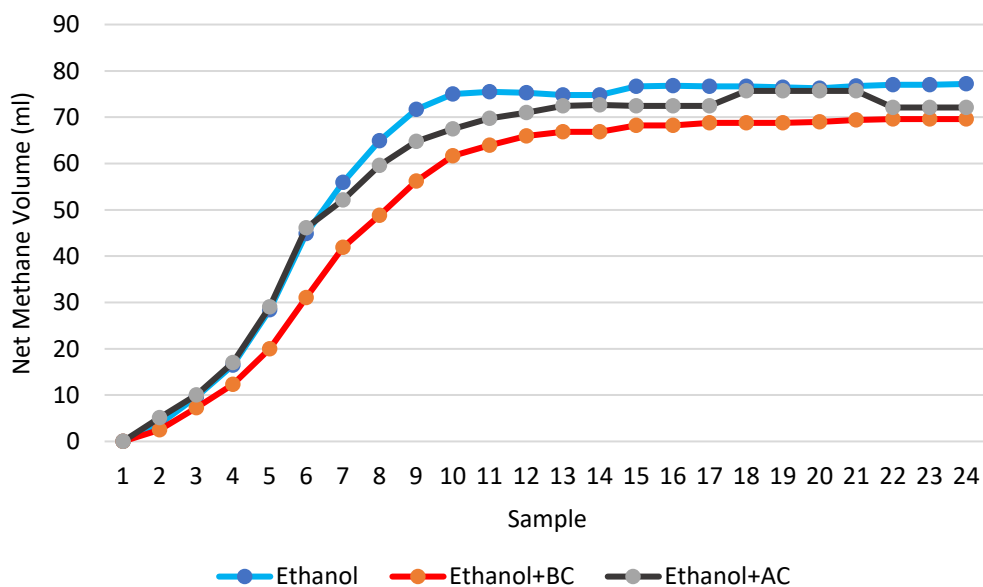
Figure 4.29: Net cumulative methane production (volume of methane after removing the effect of the negative control sample) in the second batch.
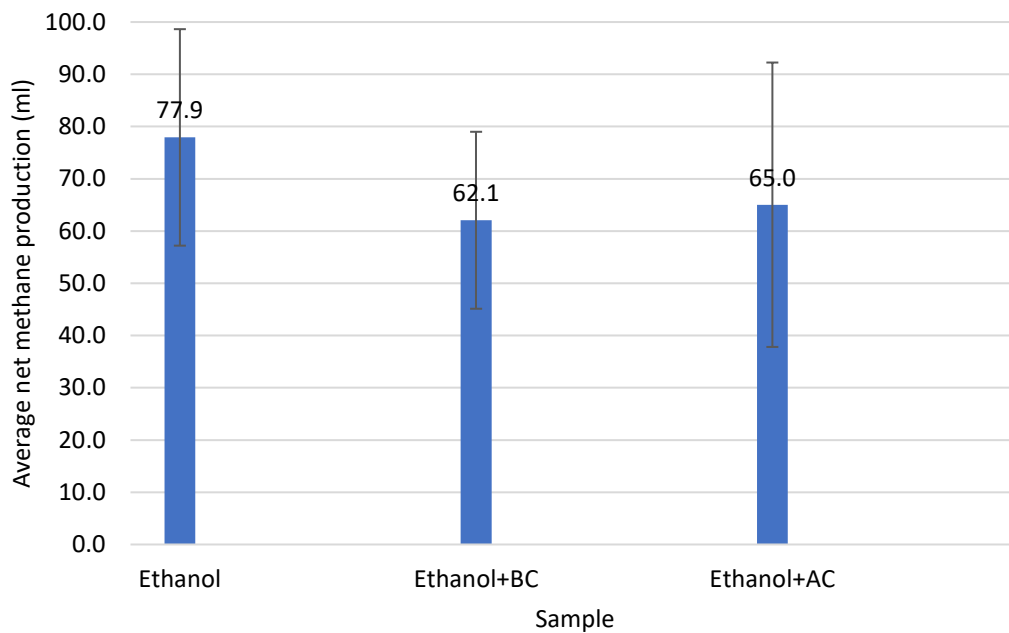
Figure 4.30: Average net cumulative methane production (volume of methane after removing the effect of the negative control) in the second batch.

Results in figures 4.29 and 4.30 are achieved by subtracting the negative control's effect and they show that adding biocarbon to methane production was not beneficial in the second feeding.
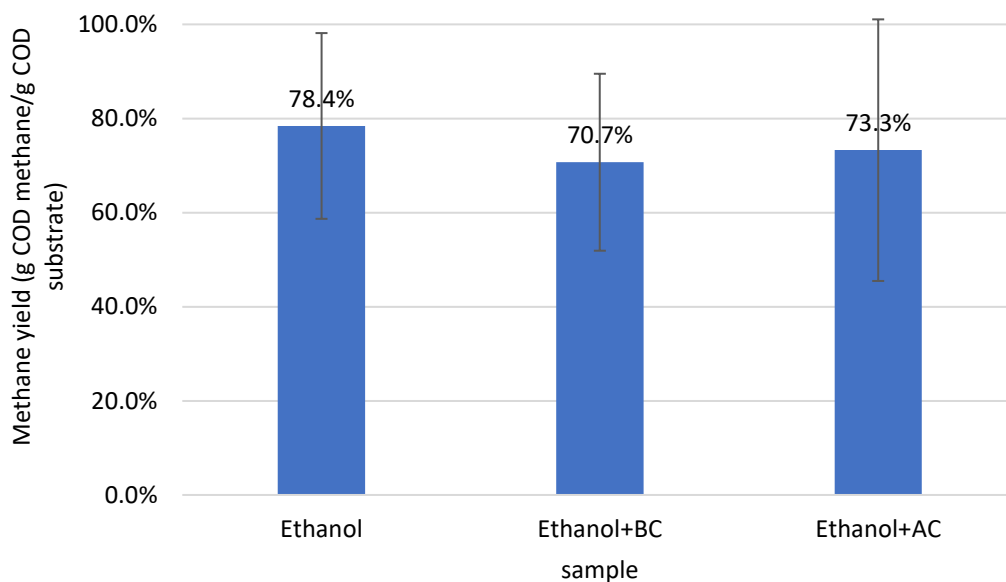
Figure 4.31: Methane yield in BMP second batch and their standard deviation with bars.

Figure 4.31 displays that in the second feeding, positive biochar and positive activated carbon declined the methane yield by 7.7% and 5.1%, respectively. Therefore, positive control had the most methane yield at 78.4%.

4.4.4 pH Variation

	Inoculum	Ino.+eth.	Ino.+eth.+BC	Ino.+BC	Ino.+eth.+AC	Ino.+AC
Day 3	8.37	8.11	8.45	8.79	8.10	8.21
Day 10	7.71	7.56	7.79	8.25	7.51	7.59
Day 17	7.58	7.44	7.74	8.08	7.41	7.54
Day 24	7.65	7.49	7.72	8.27	7.50	7.48
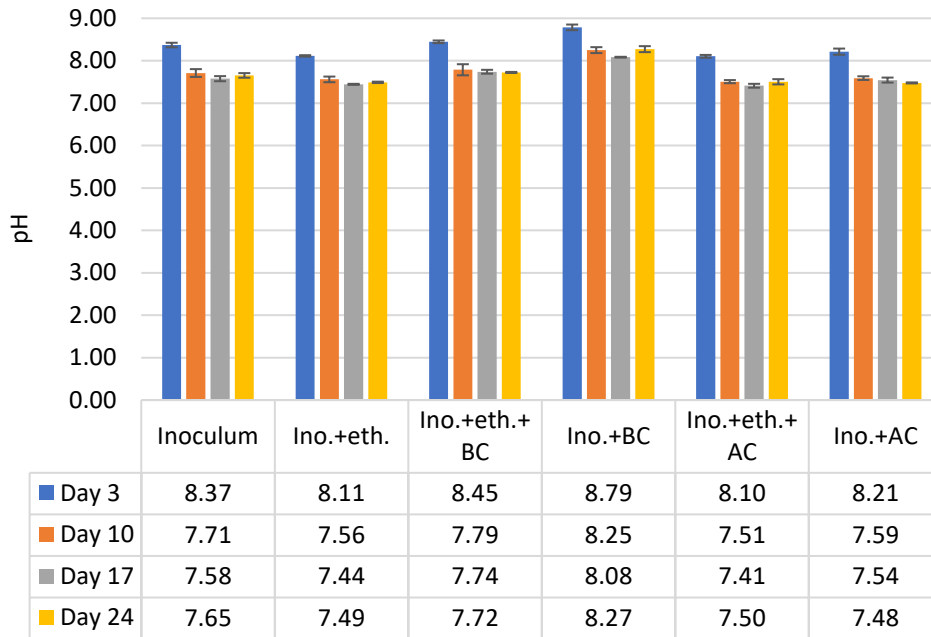
Figure 4.32: pH variation over time in different samples in the second batch and their error bars.

pH values in figure 4.32 show that generally, pH dropped after the second feeding. At the beginning of the batch, negative control biochar and positive biochar had the highest pH (8.27 and 7.72, respectively). Also, at the end of the batch, they had more pH than the other samples (8.27 and 7.72, respectively). In contrast, the addition of activated carbon did not change it noticeably, in comparison with negative control and positive control. They all dropped to less than 7.7.

4.4.5 COD
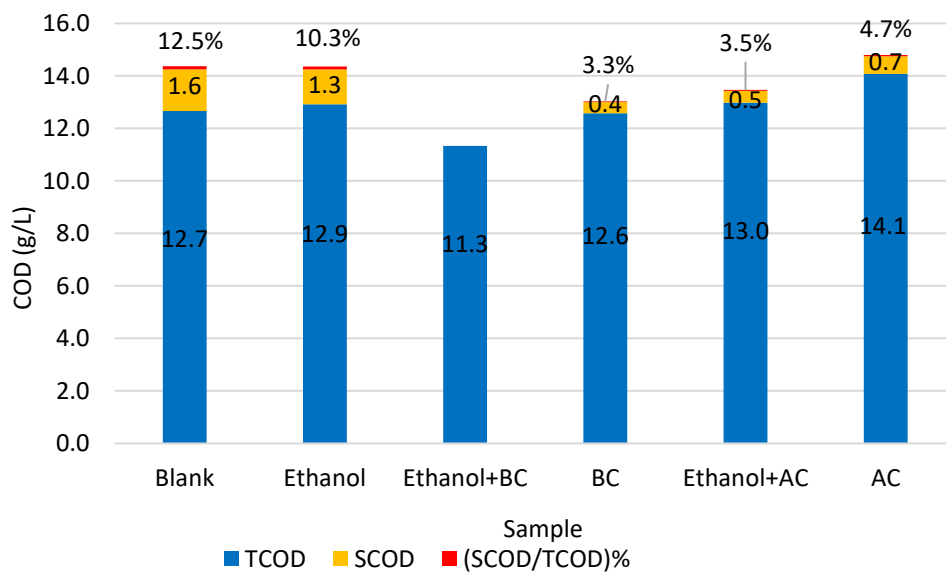
Figure 4.33: Concentration of TCOD, SCOD, and percentage of SCOD at the end of the second batch.

Regarding figure 4.33, positive biochar had the lowest concentration of TCOD (11.3 g/L), and negative control activated carbon had the most TCOD (14.1 g/L). This value in other samples was around 13 g/L. The concentration of SCOD and its percentage were higher in the negative control (1.6 g/L and 12.5%) and positive control (1.3 and 10.3%). But in addition of biocarbon, SCOD was less than 1 g/L. Therefore, its percentage was less than 5%.

4.4.6 Alkalinity
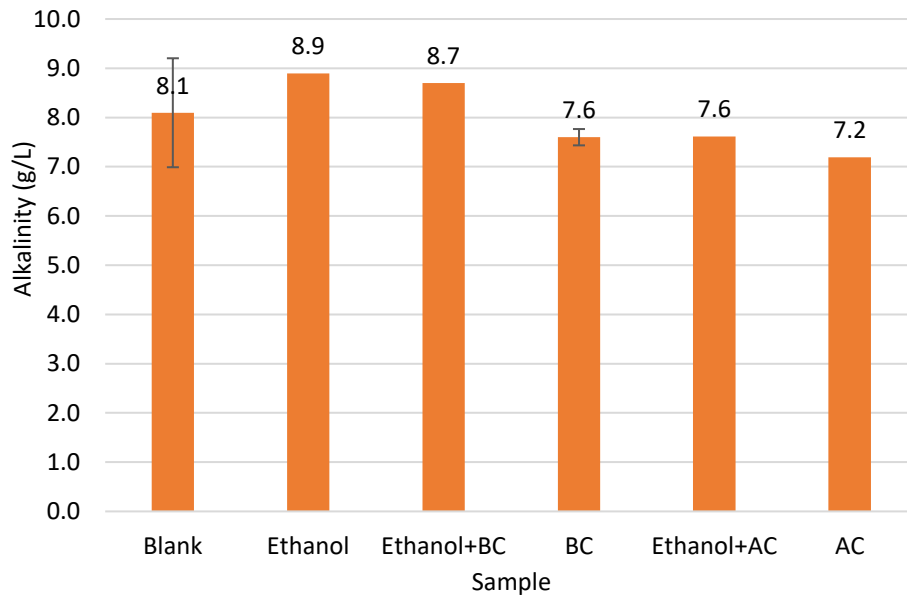
Figure 4.34: Concentration of alkalinity at the end of the second batch.

In figure 4.34 it can be seen that positive control had the highest concentration of alkalinity (8.9 g/L), while negative control activated carbon had the lowest amount (7.2 g/L). Positive biochar and positive activated carbon reduced the alkalinity from 8.9 g/L to 8.7 g/L and 7.6 g/L, respectively. Similarly, negative control biochar and negative control activated carbon declined it from 8.1 g/L in the control sample, to 7.6 g/L and 7.2 g/L, respectively.

4.4.7 Ammonium
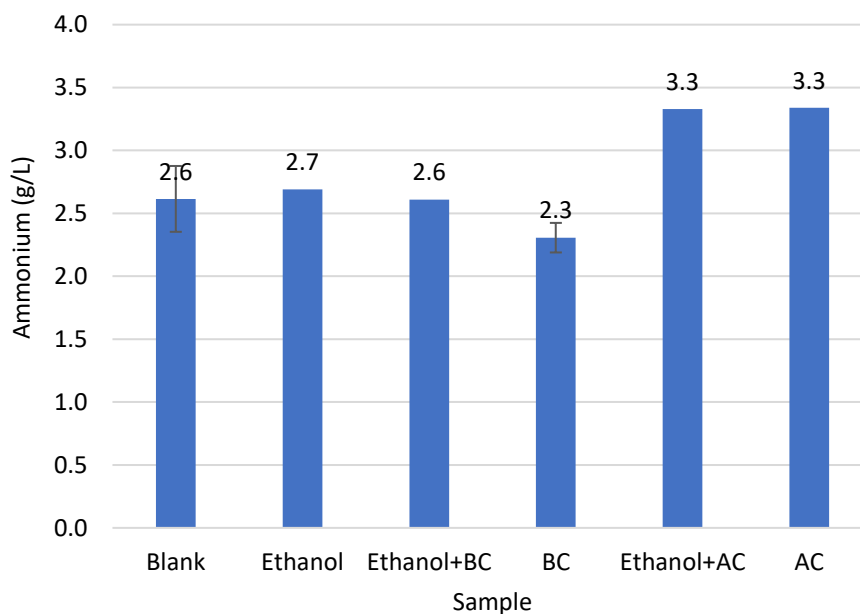
Figure 4.35: Concentration of ammonium at the end of the second batch.

According to figure 4.35, the highest concentration of ammonium was observed when activated carbon was added. It was 3.3 g/L in both negative control activated carbon and positive activated carbon. The lowest amount was in negative control biochar, which was 2.3 g/L. It can be seen that activated carbon increased the ammonium for about 0.6 g/L ((3.3-2.7)*100/3.3=18%), while positive biochar and negative control biochar decreased it for 0.1 g/L (3.7%) and 0.3 g/L ((2.6-2.3)*100/2.6=11.5%).

4.4.8 Volatile Fatty Acids
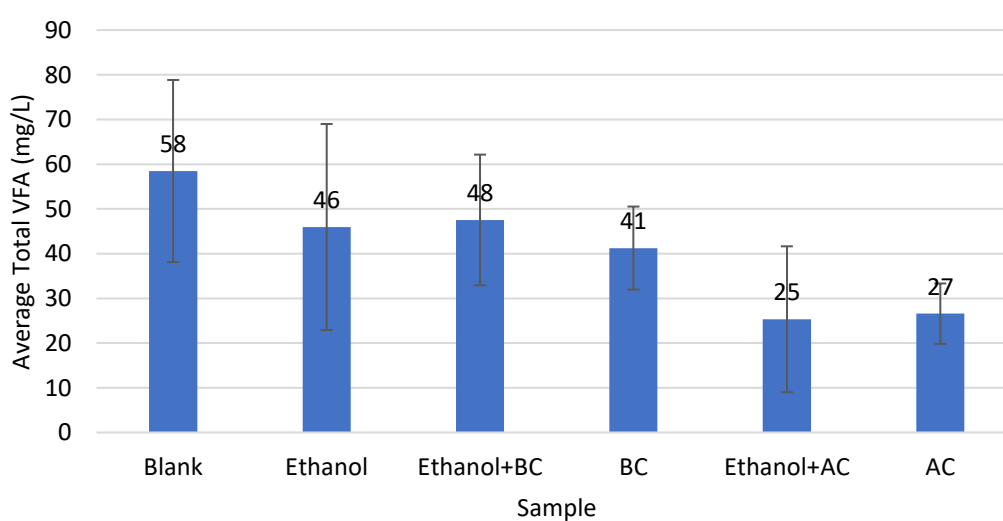
Figure 4.36: Average total volatile fatty acids at the end of the second batch.

Figure 4.36 illustrates the concentration of volatile fatty acids at the end of the second batch. The negative control sample had the highest concentration (58 mg/L), while activated carbon samples had the lowest VFA (25 and 27 mg/L in positive and negative control activated carbon, respectively). Positive biochar and negative control biochar did not change it significantly. (2 mg/L development and 17 mg/L reduction, respectively).

4.5 Biofilm formation

After the end of the BMP test, biocarbon particles were scanned by SEM to observe the microorganism attached to their surface.
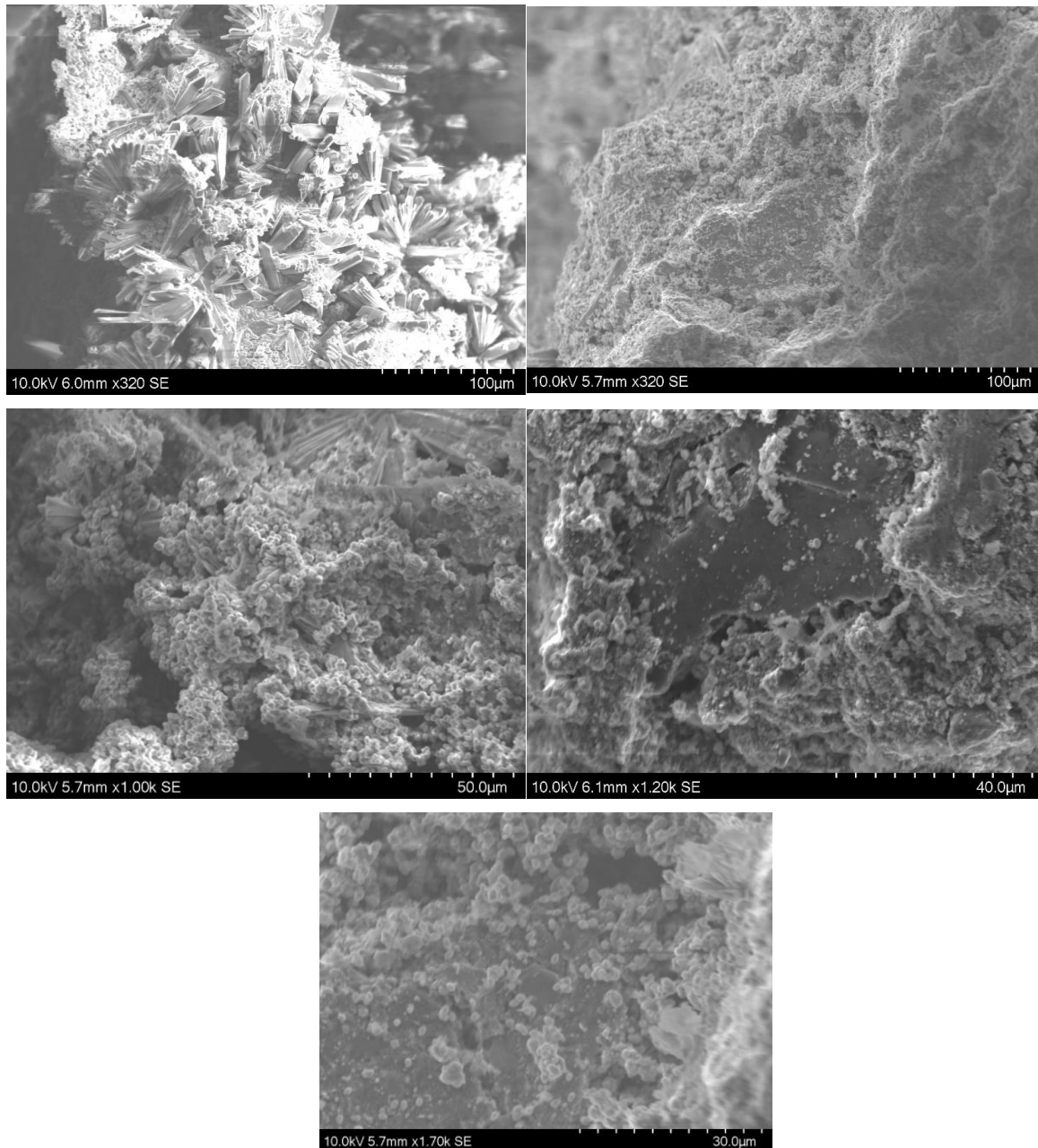
Figure 4.37: Different surfaces of the biochar particles from negative control biochar sample in dimensions of 100, 50, 40, and 30 micrometres and magnification of 320x, 1000x, 1200x, and 1700x.
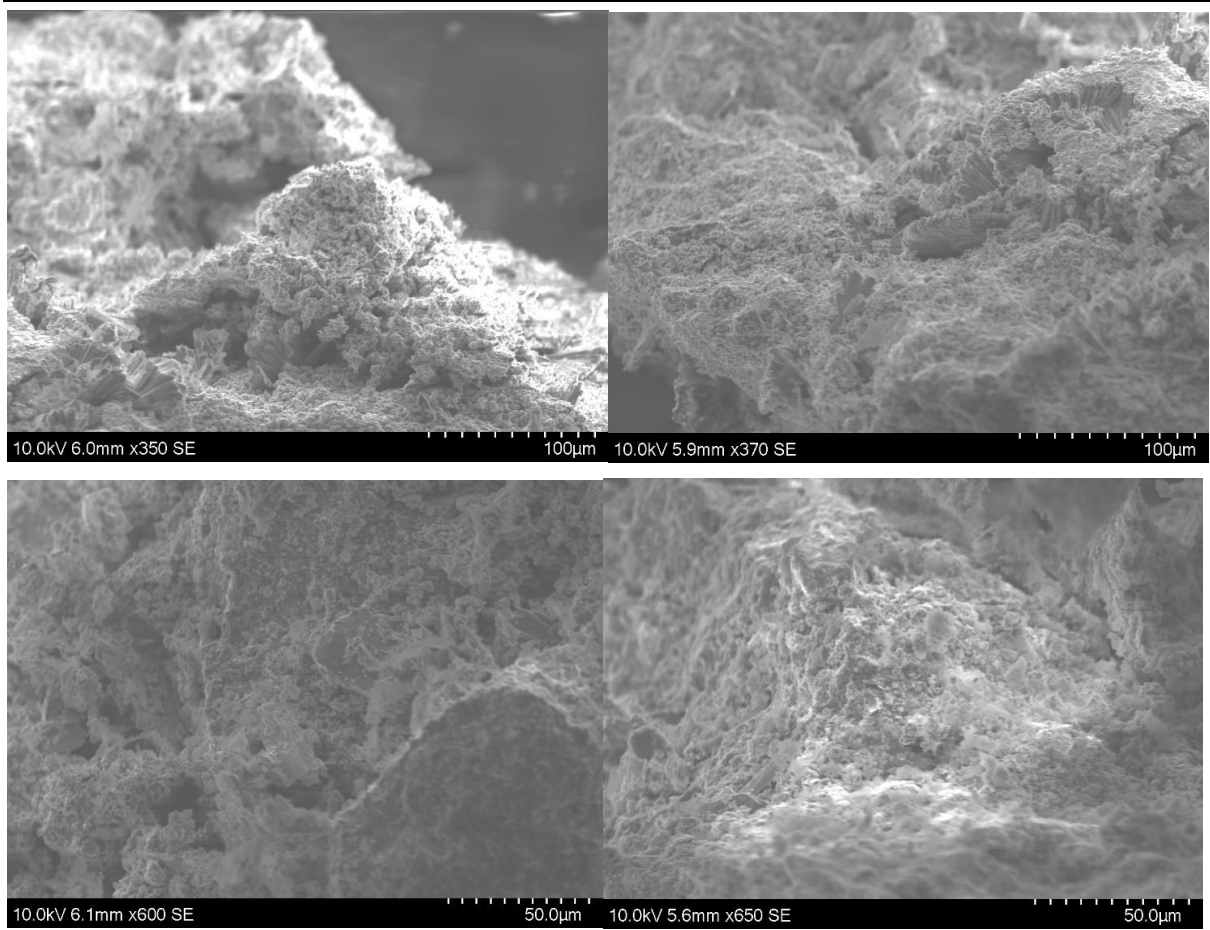
Figure 4.38: Different surfaces of the biochar particles from positive biochar sample with dimensions of 100 and 50 micrometres and magnification of 350x, 370x, 600x, and 650x.

Figures 4.37 and 4.38 shows that some compounds are attached to the surface of the biochar, however, no bacteria were found on the particles.
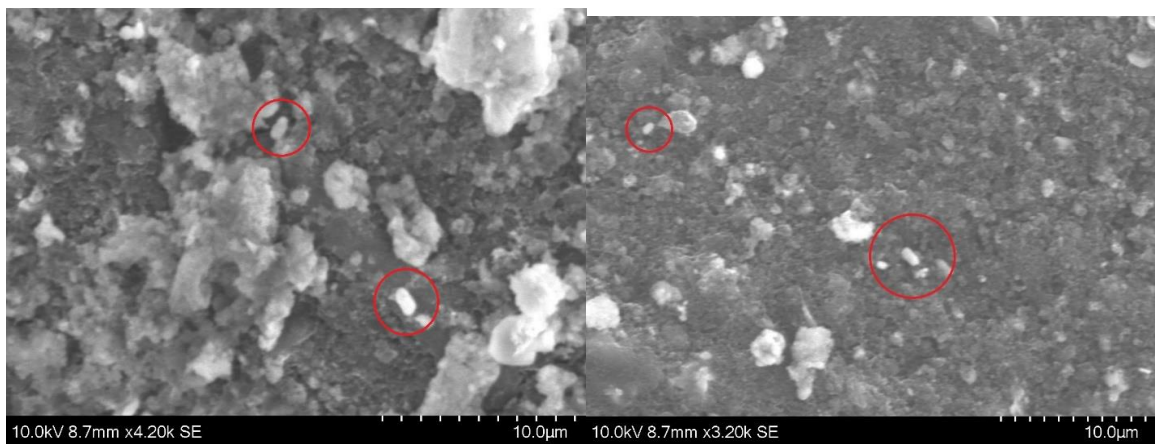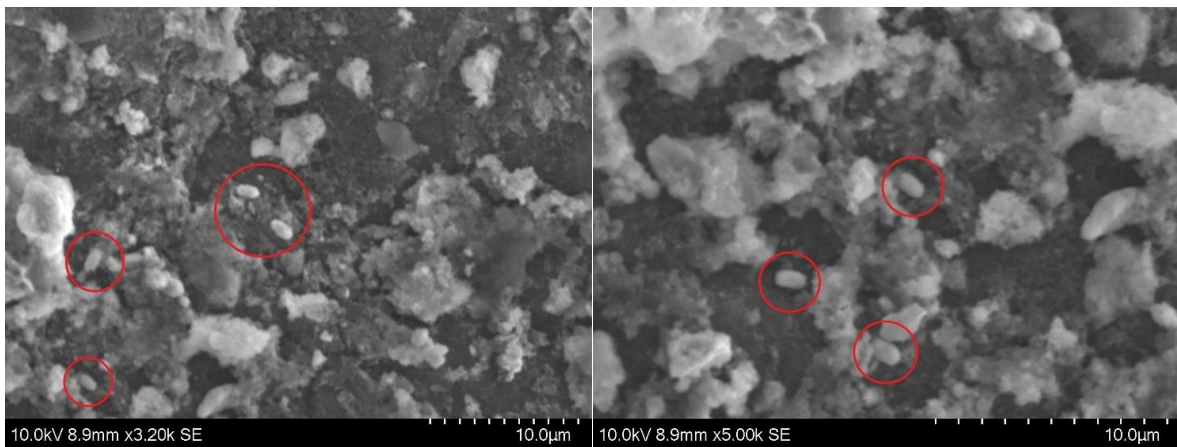
Figure 4.39: Various surfaces of the activated carbon particles from negative control activated carbon sample with dimensions of 10 micrometres and magnifications of 4200x, 3200x, and 5000x.

The red circles in figure 4.39 illustrate bacteria attached to the surface of the activated carbon particles, which were in negative control activated carbon samples. Besides bacteria, some other compounds are attached to the surface, as well.
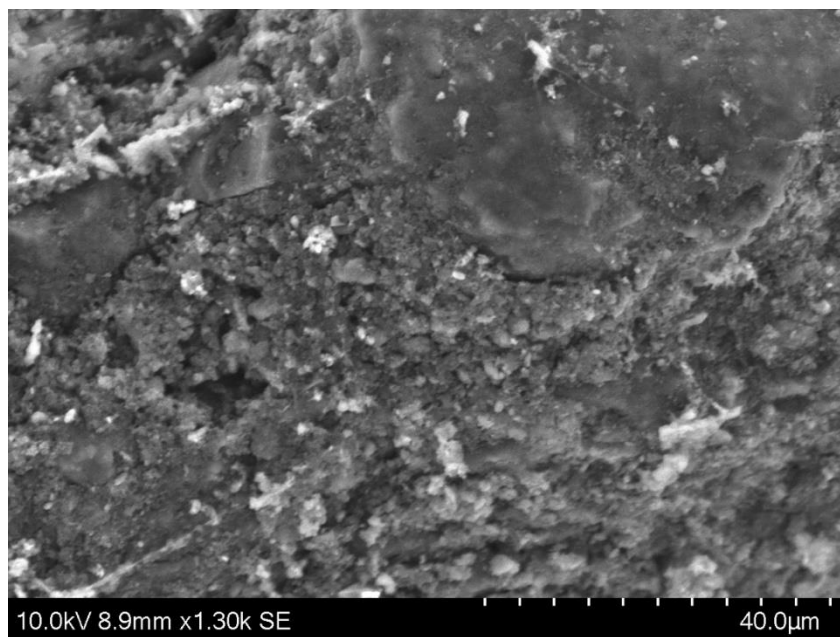
Figure 4.40: Surface of the activated carbon particle from positive activated carbon sample with dimension and magnification of 40 micrometres and 1300x, respectively.

From figure 4.40 some compounds can be seen attached to the surface, but no bacteria were observed on the activated carbon particles that were in the positive activated carbon sample.

5 Discussion

The addition of biocarbon to anaerobic digesters had some advantages and disadvantages, due to their various qualities. In this chapter, the important contributing factors to the observations are discussed.

5.1 Effect of Biocarbon on Biogas and Methane Production

It was expected that by adding biocarbon as conductive materials, more biogas will be produced [15]. Figure 4.8 shows a small improvement in the addition of activated carbon in the first feeding. Compared with the positive control, the overall biogas production increased by 3.5%. It may indicate that activated carbon also stimulates the degradation of the background substrate.

Contradictory, biochar did not show a similar effect compared with the activated carbon. This could illustrate that the DIET phenomenon is different when different material is applied in anaerobic digestion. The test result demonstrated that biochar has shown negatively, 19.4% and 52.8% reduction of biogas production by positive biochar and negative biochar control, respectively, compared to the positive and negative control in the first batch (figure 4.8).

One reason for the biochar effect can be pH development. When biochar was present, pH increased continuously in the first feeding and reached 8.57 and 8.74 in positive and control biochar, respectively (figure 4.18). Since optimum pH is below 8 this could have inhibited the microbial conditions. The pH development for the samples without biochar was less. [31] [32]
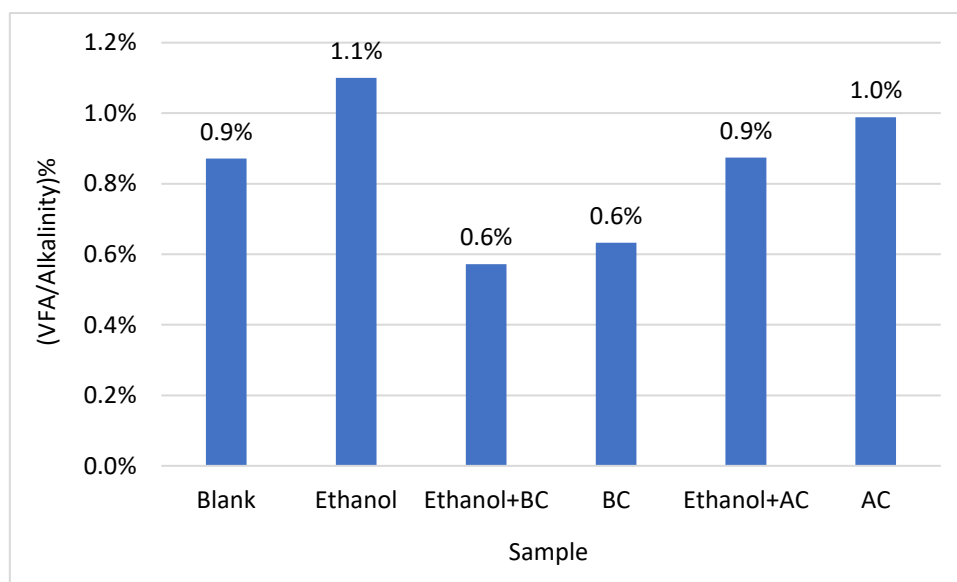
Figure 5.1: VFA to alkalinity ratio at the end of the first batch.

Figure 5.1 illustrates that samples with biochar had the lowest volatile fatty acids to alkalinity ratio (0.6%) [28][73], which resulted in higher pH. The capacity of volatile fatty acids adsorption by biochar may lead to the lower concentration of VFA and more buffering capacity [55]. Similarly, the addition of fruitwoods biochar, manure-derived biochar, and pine sawdust biochar to mesophilic anaerobic digesters verified the reduction in the volatile fatty acids

concentration [74][75][76]. On the other hand, the positive biochar sample that produced lower biogas had the most methane percentage. Biogas is mainly consisting of methane and carbon dioxide [77]. At high pH, the CO_2 gas dissolves in the liquid and converts to HCO_3^- (bicarbonate) and CO_3^{2-} (carbonate) [78], so the relative methane percentage increases in the gas phase. Equation (5.1) shows the conversion of carbon dioxide to bicarbonate, carbonate, and hydrogen ion [31][78]. figure 5.2 shows their concentration ratio at different pH values [78].

$$CO_2 + H_2O \leftrightarrow H_2CO_3 \leftrightarrow H^+ + HCO_-^3 \leftrightarrow 2H^+ + CO_3^{2-} \qquad (5.1)$$
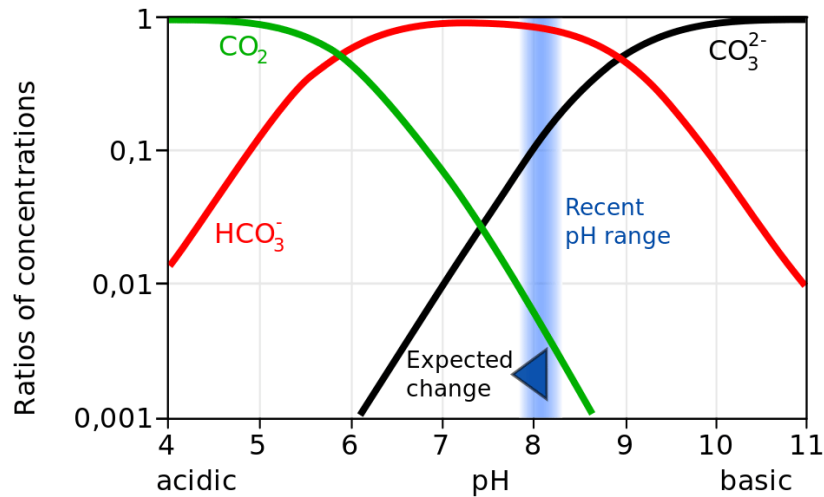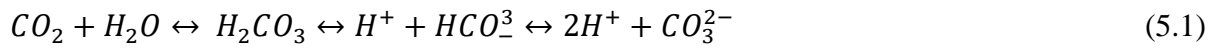
Figure 5.2: Concentration ratio of carbon dioxide, bicarbonate, and carbonate at different pH [78].
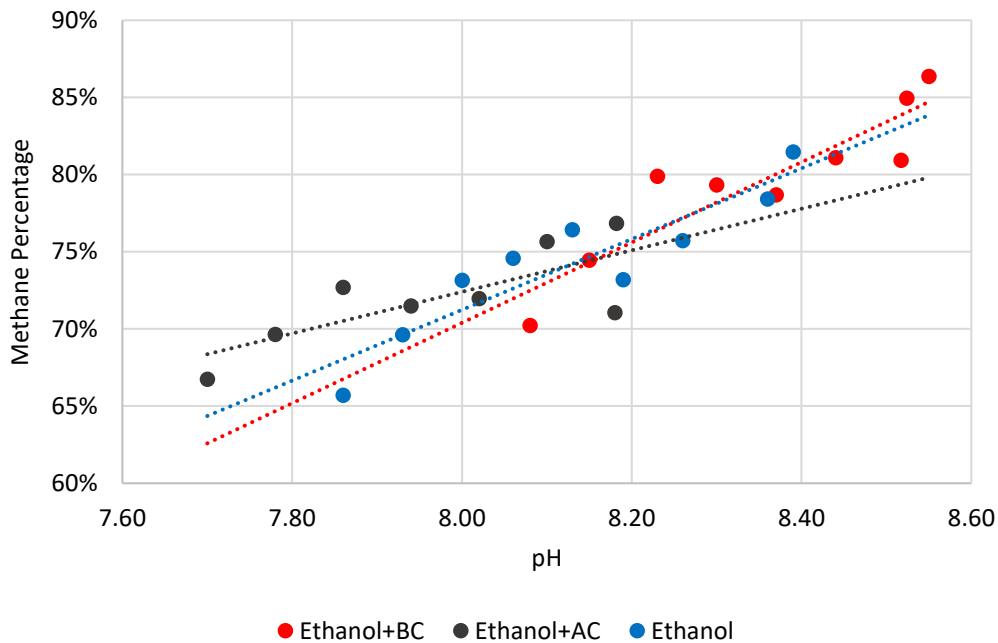
Figure 5.3: Changes in pH values and methane percentage in the positive sample in the first batch

Figure 5.3 shows increased methane percentage and pH simultaneously in the first feeding. Biochar had higher pH and higher methane percentage as well. In the second batch, the pH

decreased slowly, but biochar samples that were more alkaline had higher methane percentage (near 84%).

The same trend of variation in methane content and pH was observed in the corn stover biochar BMP test, where methane percentage increased up to more than 90% and pH was between 7.8 and 9 [79].

Although biochar improved the methane percentage, since its biogas production was lower, its methane volume was lower as well. In the first feeding positive biochar produced nearly 99 ml with a 13.9% reduction (figure 4.12).

5.2 Reusing the Conductive Materials

In this test reusing conductive particles was not profitable in terms of biogas production. It was reported that carbon conductive materials can create biofilm on their surface, which can promote the DIET phenomenon [51]. However, in this study, such an effect did not occur. It was observed in figures 4.23 and 4.24 that biocarbon reduced the biogas volume (11.5% by positive activated carbon and 21.2% by positive biochar). Even by considering the high standard deviations, they are not beneficial, while positive activated carbon acted positively in the first batch.

In section 5.1 it was discussed that high pH was one of the inhibitors in the first feeding. At the beginning of the second, although the pH started falling, figure 4.19 shows that biocarbon samples had fewer total COD and soluble COD than reactors without biocarbon. Furthermore, they had lower volatile fatty acids concentration (figure 4.21), which could have been consumed by acetogenesis and methanogenesis. Thus, less energy was provided for the bacteria to grow [28].

Positive biocarbon samples had almost the same or more methane percentage, however, their fewer biogas volume resulted in less methane volume (figures 4.27 and 4.28).

5.3 Biochar versus Activated Carbon

A previous study on similar biochar shows that its ash content is 88.4%, while the ash content of activated carbon is less than 0.4% [61][62]. Fewer ash content in activated carbon resulted in less pH development [80]. It did not reach 8.5, while biochar samples grew to more than 8.5 (figure 4.18). Thus, biogas production by activated carbon was less inhibited by pH [31][32].

The resistivity of activated carbon is 1375 $\mu\Omega$.cm and therefore its conductivity is 1/(1375*10-6)= 727.3 S/cm [62][81]. Moreover, the previous study shows that the indirect conductivity of the similar biochar in water is 0.579 mS/cm and this value for the biochar similar to the activated carbon is 1.059 mS/cm [61]. Also, according to the EDX results, biochar has 37.8% carbon and 42.7% O_2 which demonstrates oxide functional groups are present on the surface of the biochar, while activated carbon has 85.2% carbon and 11.4% oxygen (figures 4.5 and 4.6). A higher ratio of oxygen to carbon moles proves much lower conductivity in biochar [82]. Therefore, the addition of activated carbon had better potential for the development of DIET [50][83]. The conductivity of activated carbon may have been a contributing factor in the promotion of methane production in the first feeding. Not being beneficial in the second feeding shows that the addition of biocarbon to improve the DIET is only one side of the

evaluation and is not enough to achieve more efficiency in the digestion process, even if the pH of the environment is healthy for microorganisms' growth.

Furthermore, a higher surface area in activated carbon (620 m^2/g [62]) than biochar (112.76 m^2/g [61]) could mean more adsorption capacity [61]. SEM results at the end of the experiment illustrate that some compounds are attached to the surface of the biocarbon particles (figures 4.37 to 4.40). Bacteria could be observed only on the surface of the activated carbon in the absence of ethanol. No bacteria were found on the other particles' surfaces. Other studies on carbon conductive materials observed methane production promotion and bacterial communities on the surface of particles, simultaneously [84][85]. In this study, this development occurred in the negative control activated carbon. Positive activated carbon improved the methane yield, but the presence of ethanol as substrate can be a contributing factor that did not allow bacterial attachment on the surface of the particles. With the addition of biochar, no methane yield development and no interaction of microbes were observed.

Regarding the figures 4.21 and 4.36, the concentration of VFA in biochar addition reactors did not change significantly at the end of the second batch, compared to the first batch. It can be due to the limited adsorption capacity of biochar particles. They are saturated by adsorbing organic contaminants, ethanol, VFA, and some other compounds, and therefore, they could not adsorb more VFA in the second batch [10][86][87].

In this test, it has been observed that added activated carbon acted as a mediator to stimulate the direct interspecies electron transfer. Its large surface area allowed it to interact with the microbes to exchange the electrons and its higher conductivity led to minimizing the loss of electrons during the interaction with microbes. One of the previous research projects reported that the addition of activated carbon as a conductive material, stimulated the DIET phenomenon to enhance the methane production by up to 18 times compared to the control reactor [84].

Also, in previous research inhibition of methane production by biochar was observed, especially after doubling its dosage. Increasing the biochar load from 0.9 g/g-VS substrate to 1.8 g/g-VS substrate, reduced the methane yield by 12% [55].

5.4 Effect of Biocarbon on Inoculum

Regarding the biogas production results (figures 4.8 and 4.23), negative biocarbon controls acted negatively on it. However, activated carbon improved the methane percentage by 33% in the first feeding and as the result increased the methane volume to 1.1 times more than the negative control. Figure 5.1 displays that negative activated carbon control and negative control had a close ratio of VFA to alkalinity (1% and 0.9%, respectively), which resulted in almost the same pH during the digestion process (figure 4.18). Due to this similarity in pH, methane volume development shows how using activated carbon as conductive material can increase the efficiency of the methanogenesis and improve methane production. On the contrary, biochar high loading caused higher pH that counteracted its conductivity quality and thus, could not be beneficial to methane production.

6 Conclusion

The biogas production was increased by 3.5% when activated carbon was applied in the anaerobic digestion of ethanol. However, when biochar was applied in a similar system, it did not affect similarly.

With regards to the obtained results and contributing factors, it can be concluded that although biocarbon can promote biogas and methane production by being conductive, their other properties might inhibit the anaerobic digestion process. In this study, the ash content of biochar inhibited the digesters by raising the pH sharply up to 8.7. High buffering capacity in the addition of biochar, required acidic compounds accumulation to reduce the pH to lower than 8. However, its adsorption capacity did not allow it.

Also, this test indicates over time the biocarbon particles will be less effective. It might be due to the adsorption of other compounds such as organic pollutants prior to bacteria and creating a less desirable surface for microbes' attachment. Therefore, new particles should be added continuously as co-substrate to the anaerobic digesters to observe some benefits. reusing the conductive materials is not beneficial, because particles' surface adsorbs other compounds such as organic pollutants before the bacteria.

In the case of this biochar and other biochar with similar key factors such as high ash content, pH, and conductivity, a lower load of biochar should be added to the reactors to take advantage of it in biogas production by preventing pH development and negative side of acidic compounds adsorption. It is recommended not to reduce the substrate load because the biochar can adsorb it before the acidic compounds. Moreover, the pH should be measured regularly not to violate the optimum range. Generally, high oxide biochar might be more beneficial in wastewater treatment processes rather than inside bioreactors by adsorbing organic pollutants.

References

[1] "Solid waste management: Cause, effects." https://theintactone.com/2019/10/29/es-u2-topic-17-solid-waste-management-cause-effects/ (accessed May 15, 2022).

[2] "Landfills | National Geographic Society." https://www.nationalgeographic.org/encyclopedia/landfills/ (accessed May 15, 2022).

[3] "Municipal waste management across European countries," 2016. [Online]. Available: https://www.eea.europa.eu/publications/municipal-waste-management-across-european-countries

[4] "Why Anaerobic Digestion? Reasons to Support Biogas." https://biogas-digester.com/why-anaerobic-digestion (accessed May 15, 2022).

[5] M. A. Bhat, A. W. Adil, B. M. Sikander, Y. Lone, and J. A. Malik, "Waste Management Technology for Sustainable Agriculture," in *innovative waste management technologies for sustainable development*, no. September, IGI GLOBAL PUBLISER OF TIMELY KNOWLEDE, 2019, pp. 156–176. doi: 10.4018/978-1-7998-0031-6.ch009.

[6] "Pyrolysis of Municipal Wastes | BioEnergy Consult." https://www.bioenergyconsult.com/pyrolysis-of-municipal-waste/ (accessed May 09, 2022).

[7] K. Zhu, X. Wang, D. Chen, W. Ren, H. Lin, and H. Zhang, "Wood-based biochar as an excellent activator of peroxydisulfate for Acid Orange 7 decolorization.," *Chemosphere*, vol. 231, pp. 32–40, Sep. 2019, doi: 10.1016/j.chemosphere.2019.05.087.

[8] X. Zhang, P. Zhang, X. Yuan, Y. Li, and L. Han, "Effect of pyrolysis temperature and correlation analysis on the yield and physicochemical properties of crop residue biochar," *Bioresour. Technol.*, vol. 296, no. September 2019, p. 122318, 2020, doi: 10.1016/j.biortech.2019.122318.

[9] S. J.Taherzadeh, Mohammad (Swedish Centre for Resource Recovery, University of Borås, Borås, S. Bolton, Kim (Swedish Centre for Resource Recovery, University of Borås, Borås, C. Wong, Jonathan (Institute of Bioresource and Agriculture, Hong Kong Baptist University, Kowloon Tong, Hong Kong, and I. Pandey, Ashok (Centre for Innovation and Translational Research, CSIR-Indian Institute of Toxicology Research, Lucknow, Eds., "Influential Aspects in Waste Management Practices," in *Sustainable Resource Recovery and Zero Waste Approaches*, Elsevier, 2019. doi: https://doi.org/10.1016/C2017-0-04415-4.

[10] M. Chiappero *et al.*, "Review of biochar role as additive in anaerobic digestion processes," *Renew. Sustain. Energy Rev.*, vol. 131, no. October 2019, 2020, doi: 10.1016/j.rser.2020.110037.

[11] M. Derek R. Lovley (Department of Microbiology, University of Massachusetts, Amherst, "Syntrophy Goes Electric: Direct Interspecies Electron Transfer," *Annu. Rev. Microbiol.*, pp. 71:643–64, 2017, doi: https://doi.org/10.1146/annurev-micro-030117-020420.

[12] "Anaerobic Digestion (AD) A Renewable Energy Technology."
      https://www.powersystemsuk.co.uk/anaerobic-digestion/anaerobic-digestion-
      renewable-energy-technology/ (accessed May 15, 2022).

[13] L. Chen and H. Neibling, "Anaerobic Digestion Basics." University of Idaho, 2014.

[14] A. Mostafa, S. Im, Y. C. Song, Y. Ahn, and D. H. Kim, "Enhanced anaerobic digestion
      by stimulating DIET reaction," *Processes*, vol. 8, no. 4, pp. 1–17, 2020, doi:
      10.3390/PR8040424.

[15] W. Zhao, H. Yang, S. He, Q. Zhao, and L. Wei, "A review of biochar in anaerobic
      digestion to improve biogas production: Performances, mechanisms and economic
      assessments," *Bioresour. Technol.*, vol. 341, no. June, p. 125797, 2021, doi:
      10.1016/j.biortech.2021.125797.

[16] Y. Nalinga and I. Legonda, "The effect of particles size on biogas production," *Int. J.
      Innov. Res. Technol. Sci.*, vol. 4, no. 2, pp. 9–13, 2016, [Online]. Available:
      http://repository.udom.ac.tzhttp//hdl.handle.net/20.500.12661/2133

[17] L. Zhang *et al.*, "Biochar enhanced thermophilic anaerobic digestion of food waste:
      Focusing on biochar particle size, microbial community analysis and pilot-scale
      application," *Energy Convers. Manag.*, vol. 209, no. January, p. 112654, 2020, doi:
      10.1016/j.enconman.2020.112654.

[18] N. Aryal, Y. Zhang, S. Bajracharya, D. Pant, and X. Chen, "Microbial electrochemical
      approaches of carbon dioxide utilization for biogas upgrading," *Chemosphere*, vol.
      291, no. P1, p. 132843, 2022, doi: 10.1016/j.chemosphere.2021.132843.

[19] N. Aryal, M. Odde, C. Bøgeholdt Petersen, L. Ditlev Mørck Ottosen, and M. Vedel
      Wegener Kofoed, "Methane production from syngas using a trickle-bed reactor setup,"
      Bioresour. Technol., vol. 333, 2021, doi: 10.1016/j.biortech.2021.125183.

[20] "Anaerobic Digestion - Definition, Process, Advantages and Treatment."
      https://www.vedantu.com/biology/anaerobic-
      digestion?msclkid=b525d71ccfba11ec9e512885f70eca8f (accessed May 09, 2022).

[21] "How Does Anaerobic Digestion Work? | US EPA." https://www.epa.gov/agstar/how-
      does-anaerobic-digestion-work?msclkid=e7b7552dcfba11ecb6c3fd8fb2436a32
      (accessed May 09, 2022).

[22] "Anaerobic digestion: What is it and how does it work?"
      https://climate.selectra.com/en/recycling/anaerobic-
      digestion?msclkid=2c94a07ccfbb11ec9b0806dda52f46d6 (accessed May 09, 2022).

[23] "Basic Information about Anaerobic Digestion (AD) | Anaerobic Digestion (AD) | US
      EPA." https://19january2021snapshot.epa.gov/anaerobic-digestion/basic-information-
      about-anaerobic-digestion-ad_.html?msclkid=5757f07ccfbb11ec986b6a3a6d25c011
      (accessed May 09, 2022).

[24] "Iona Capital | UK Low Carbon Fund Manager."
      https://ionacapital.co.uk/?msclkid=0e85e471cfbc11ecb84f204049a4b16b (accessed
      May 09, 2022).

[25] N. Aryal, T. Kvist, F. Ammam, D. Pant, and L. D. M. Ottosen, "An overview of
      microbial biogas enrichment," *Bioresour. Technol.*, vol. 264, no. April, pp. 359–369,
      2018, doi: 10.1016/j.biortech.2018.06.013.

[26] N. Aryal and T. Kvist, "Alternative of biogas injection into the Danish gas grid system—a study from demand perspective," *ChemEngineering*, vol. 2, no. 3, pp. 1–11, 2018, doi: 10.3390/chemengineering2030043.

[27] J. Fernández-Rodríguez, M. Pérez, and L. I. Romero, "Semicontinuous Temperature-Phased Anaerobic Digestion (TPAD) of Organic Fraction of Municipal Solid Waste (OFMSW). Comparison with single-stage processes," *Chem. Eng. J.*, vol. 285, pp. 409–416, 2016, doi: 10.1016/j.cej.2015.10.027.

[28] Metcalf & Eddy, *Wastewater Engineering Wastewater Engineering Treatment and Resource Recovery*, Fifth. 2014.

[29] "Mesophilic Anaerobic Digestion." https://anaerobic-digestion.com/the-anaerobic-digestion-process/mesophilic-anaerobic-digestion/?msclkid=55207a7ccfc011ecb5ec7c979bb997c5 (accessed May 09, 2022).

[30] J. del Real Olvera and A. Lopez-Lopez, "Biogas Production from Anaerobic Treatment of Agro-Industrial Wastewater," *Biogas*, no. March, 2012, doi: 10.5772/31906.

[31] "Alkalinity and pH - Anaerobic Digesters - Flanders Health Blog." https://www.flandershealth.us/anaerobic-digesters/alkalinity-and-ph.html?msclkid=0fe12bb5cfc111ecab53db8bf3dc2b87 (accessed May 09, 2022).

[32] A. E. Cioabla, I. Ionel, G. A. Dumitrel, and F. Popescu, "Comparative study on factors affecting anaerobic digestion of agricultural vegetal residues," *Biotechnol. Biofuels*, vol. 5, no. 1, p. 1, 2012, doi: 10.1186/1754-6834-5-39.

[33] O. Yenigün and B. Demirel, "Ammonia inhibition in anaerobic digestion: A review," *Process Biochem.*, vol. 48, no. 5–6, pp. 901–911, 2013, doi: 10.1016/j.procbio.2013.04.012.

[34] R. C.Ray, *Sustainable Biofuels Opportunities and Challenges*. Academic Press, 2021. doi: https://doi.org/10.1016/C2019-0-01185-5.

[35] P. L. McCarty and R. E. McKinney, "Salt Toxicity in Anaerobic Digestion on JSTOR," *Water Pollut. Control Fed.*, vol. 33, no. 4, pp. 399–415, [Online]. Available: http://www.jstor.org/stable/25034396

[36] "What is pyrolysis process?" https://www.biogreen-energy.com/what-is-pyrolysis?msclkid=9ba859e4cfc611eca1fda1b1ecafbb9c (accessed May 09, 2022).

[37] "What is Pyrolysis? : USDA ARS." https://www.ars.usda.gov/northeast-area/wyndmoor-pa/eastern-regional-research-center/docs/biomass-pyrolysis-research-1/what-is-pyrolysis/?msclkid=5808af4ccfc711ecbc8ccb659deb9163 (accessed May 09, 2022).

[38] N. B. K. Rasmussen and N. Aryal, "Syngas production using straw pellet gasification in fluidized bed allothermal reactor under different temperature conditions," *Fuel*, vol. 263, no. May, 2020, doi: 10.1016/j.fuel.2019.116706.

[39] "Biomass Pyrolysis Process | BioEnergy Consult." https://www.bioenergyconsult.com/biomass-pyrolysis-process/?msclkid=b3396c1ecfc711ecb4f4f5eb605be672 (accessed May 09, 2022).

[40] S. K. Ning, M. C. Hung, Y. H. Chang, H. P. Wan, H. T. Lee, and R. F. Shih, "Benefit

assessment of cost, energy, and environment for biomass pyrolysis oil," *J. Clean. Prod.*, vol. 59, pp. 141–149, 2013, doi: 10.1016/j.jclepro.2013.06.042.

[41] L. Axelsson, M. Franzén, M. Ostwald, G. Berndes, G. Lakshmi, and N. H. Ravindranath, "Perspective: Jatropha cultivation in southern India: Assessing farmers' experiences," *Biofuels, Bioprod. Biorefining*, vol. 6, no. 3, pp. 246–256, 2012, doi: 10.1002/bbb.

[42] K. Qian, A. Kumar, H. Zhang, D. Bellmer, and R. Huhnke, "Recent advances in utilization of biochar," *Renew. Sustain. Energy Rev.*, vol. 42, pp. 1055–1064, 2015, doi: 10.1016/j.rser.2014.10.074.

[43] J. Lehmann, M. C. Rillig, J. Thies, C. A. Masiello, W. C. Hockaday, and D. Crowley, "Biochar effects on soil biota - A review," *Soil Biol. Biochem.*, vol. 43, no. 9, pp. 1812–1836, 2011, doi: 10.1016/j.soilbio.2011.04.022.

[44] M. Ahmad *et al.*, "Biochar as a sorbent for contaminant management in soil and water: A review," *Chemosphere*, vol. 99, pp. 19–33, 2014, doi: 10.1016/j.chemosphere.2013.10.071.

[45] A. S. González, M. G. Plaza, F. Rubiera, and C. Pevida, "Sustainable biomass-based carbon adsorbents for post-combustion CO2 capture," *Chem. Eng. J.*, vol. 230, pp. 456–465, 2013, doi: 10.1016/j.cej.2013.06.118.

[46] N. Q. Zaman, "THE APPLICABILITY OF BATCH TESTS TO ASSESS BIOMETHANATION POTENTIAL OF ORGANIC WASTE AND ASSESS SCALE UP TO CONTINUEOUS REACTOR SYSTEMS," University of Canterbury, 2010.

[47] J. Filer, H. H. Ding, and S. Chang, "Biochemical Methane Potential (BMP) Assay Method for Anaerobic Digestion Research," *Water*, vol. 11, no. 921, 2019, doi: 10.3390/w11050921.

[48] A. Rozzi and E. Remigi, "Methods of assessing microbial activity and inhibition under anaerobic," *Rev. Environ. Sci. Bio/Technology*, no. 3, pp. 93–115, 2004, doi: https://doi.org/10.1007/s11157-004-5762-z.

[49] A. J. Guwy, "Equipment used for testing anaerobic biodegradability and activity," *Rev. Environ. Sci. Bio/Technology*, 2004, doi: https://doi.org/10.1007/s11157-004-1290-0.

[50] P. Gahlot *et al.*, "Conductive material engineered direct interspecies electron transfer (DIET) in anaerobic digestion: Mechanism and application," *Environ. Technol. Innov.*, vol. 20, p. 101056, 2020, doi: 10.1016/j.eti.2020.101056.

[51] R. D. A. Cayetano *et al.*, "Biofilm formation as a method of improved treatment during anaerobic digestion of organic matter for biogas recovery," *Bioresour. Technol.*, vol. 344, no. PB, p. 126309, 2022, doi: 10.1016/j.biortech.2021.126309.

[52] Y. Liu, X. Li, S. Wu, Z. Tan, and C. Yang, "Enhancing anaerobic digestion process with addition of conductive materials," *Chemosphere*, vol. 278, p. 130449, 2021, doi: 10.1016/j.chemosphere.2021.130449.

[53] H. J. Kang *et al.*, "Recent advances in methanogenesis through direct interspecies electron transfer via conductive materials: A molecular microbiological perspective," *Bioresour. Technol.*, vol. 322, no. December 2020, 2021, doi: 10.1016/j.biortech.2020.124587.

[54] Z. Zhao, Y. Zhang, Y. Li, Y. Dang, T. Zhu, and X. Quan, "Potentially shifting from interspecies hydrogen transfer to direct interspecies electron transfer for syntrophic metabolism to resist acidic impact with conductive carbon cloth," *Chem. Eng. J.*, vol. 313, pp. 10–18, 2017, doi: 10.1016/j.cej.2016.11.149.

[55] C. Cimon, "Effect of biochar and wood ash amendment on biochemical methane production of wastewater sludge from a temperature phase anaerobic digestion process," THE UNIVERSITY OF BRITISH COLUMBIA, 2020.

[56] "What do we do? • Lindum." https://lindum.no/hva-gjor-vi/?msclkid=c1d22a28cfcd11ec8036727cf7b8408f (accessed May 09, 2022).

[57] V. Sivalingam and C. Dinamarca, "High pressure moving bed biofilm reactor for syngas fermentation," *Chem. Eng. Trans.*, vol. 86, no. April, pp. 1483–1488, 2021, doi: 10.3303/CET2186248.

[58] A. G. Tesfay, K. Kassa, and D. Reddythota, "Determination of Bio-methane Potential as Renewable Energy of Beverage Industrial Effluents at Mekelle, Ethiopia," *Adv. Sci. Technol.*, vol. 385, no. July, pp. 69–84, 2021, doi: https://doi.org/10.1007/978-3-030-80618-7_5.

[59] V. Sivalingam, V. Ahmadi, O. Babafemi, and C. Dinamarca, "Integrating syngas fermentation into a single-cell microbial electrosynthesis (MES) reactor," *Catalysts*, vol. 11, no. 1, pp. 1–10, 2021, doi: 10.3390/catal11010040.

[60] "US Patent for Heating worm conveyor Patent (Patent # 6,375,345 issued April 23, 2002) - Justia Patents Search." https://patents.justia.com/patent/6375345 (accessed May 15, 2022).

[61] Y. Dzihora, "Biochar from organic waste: characterization and use," Norwegian University of Life Sciences, 2021.

[62] "Activated charcoal DARCO, particle size 20-40mesh, granular 7440-44-0." https://www.sigmaaldrich.com/NO/en/product/sigald/242268?msclkid=9f90468bd04811ecb84baee3a9499381 (accessed May 10, 2022).

[63] N. Aryal *et al.*, "Increased carbon dioxide reduction to acetate in a microbial electrosynthesis reactor with a reduced graphene oxide-coated copper foam composite cathode," *Bioelectrochemistry*, vol. 128, pp. 83–93, 2019, doi: 10.1016/j.bioelechem.2019.03.011.

[64] C. Holliger, S. Astals, H. F. de Laclos, S. D. Hafner, K. Koch, and S. Weinrich, "Towards a standardization of biomethane potential tests: A commentary," *Water Sci. Technol.*, vol. 83, no. 1, pp. 247–250, 2021, doi: 10.2166/wst.2020.569.

[65] "Water, Food and Environmental Analytics Catalog | Analytics & Sample Prep | Merck." https://www.merckmillipore.com/NO/en/20170308_183420?ReferrerURL=https%3A%2F%2Fwww.bing.com%2F&msclkid=64a6c41bd03011ec9e567f7f7381a8d2 (accessed May 10, 2022).

[66] "International Water Association - International Water Association." https://iwa-network.org/?msclkid=d190d954d03011ec88031044b581a0d1 (accessed May 10, 2022).

[67] "Merck | Norway."

https://www.sigmaaldrich.com/NO/en?msclkid=40fe2429d03111ecbf335b0bd0d724e9 (accessed May 10, 2022).

[68] "SQ Prove 100 - Analytical Procedures and Appendices 2017-07 | PDF | Spectrophotometry | Chromium." https://www.scribd.com/document/517366705/SQ-Prove-100-Analytical-Procedures-and-Appendices-2017-07?msclkid=64645589d03111ecbe33954c1c6b34e2 (accessed May 10, 2022).

[69] "Water, Food and Environmental Analytics Catalog | Analytics & Sample Prep | Merck." https://www.merckmillipore.com/NO/en/20170308_183420?ReferrerURL=https%3A%2F%2Fwww.bing.com%2F&msclkid=ad3bfbfdd03111ec910ed254dcbc8f95 (accessed May 10, 2022).

[70] E. and A. D. A. Telliard, William (U.S Environmental Protection Agency's Office of Water, "Method 1684 Total, Fixed, and Volatile Solids.pdf." 2001.

[71] B. Zhu, P. Gikas, R. Zhang, J. Lord, B. Jenkins, and X. Li, "Characteristics and biogas production potential of municipal solid wastes pretreated with a rotary drum reactor," *Bioresour. Technol.*, vol. 100, no. 3, pp. 1122–1129, 2009, doi: 10.1016/j.biortech.2008.08.024.

[72] B. Singh, M. M. Dolk, Q. Shen, and M. Camps-Arbestain, "Biochar pH, electrical conductivity and liming potential," in *Biochar: A Guide to Analytical Methods*, no. June 2018, CSIRO Publishing, 2017, pp. 23–38. [Online]. Available: https://ebooks.publish.csiro.au/content/ISBN/9781486305100

[73] I. Hamawand and C. Baillie, "Anaerobic digestion and biogas potential: Simulation of lab and industrial-scale processes," *Energies*, vol. 8, no. 1, pp. 454–474, 2015, doi: 10.3390/en8010454.

[74] J. Cai, P. He, Y. Wang, L. Shao, and F. Lu, "Effects and optimization of the use of biochar in anaerobic digestion of food wastes," *Waste Manag. Res.*, pp. 409–416, 2016, doi: 10.1177/0734242X16634196.

[75] H. M. Jang, Y.-K. Choi, and E. Kan, "Effects of dairy manure-derived biochar on psychrophilic, mesophilic and thermophilic anaerobic digestions of dairy manure," *Bioresour. Technol.*, vol. 250, no. November 2017, pp. 927–931, 2018, doi: 10.1016/j.biortech.2017.11.074.

[76] N. M. S. Sunyoto, M. Zhu, Z. Zhang, and D. Zhang, "Effect of biochar addition on hydrogen and methane production in two-phase anaerobic digestion of aqueous carbohydrates food waste," *Bioresour. Technol.*, vol. 219, pp. 29–36, 2016, doi: 10.1016/j.biortech.2016.07.089.

[77] "What Is Biogas? - What Is Biogas?" https://ezratmp-qws1u.gitbook.io/what-is-biogas/?msclkid=97da6f9cd04611ecb95f0b0aa419c5fe (accessed May 10, 2022).

[78] P. Webb, "5.5 Carbon Dioxide, pH, and Ocean Acidification," in *Introduction to Oceanography*, 2019. [Online]. Available: http://rwu.pressbooks.pub/webboceanography Cover

[79] Y. Shen, J. L. Linville, M. Urgun-Demirtas, R. P. Schoene, and S. W. Snyder, "Producing pipeline-quality biomethane via anaerobic digestion of sludge amended with corn stover biochar with in-situ CO2 removal," *Appl. Energy*, vol. 158, pp. 300–

309, 2015, doi: 10.1016/j.apenergy.2015.08.016.

[80] S. O. Masebinu, E. T. Akinlabi, E. Muzenda, and A. O. Aboyade, "A review of biochar properties and their roles in mitigating challenges with anaerobic digestion," *Renew. Sustain. Energy Rev.*, vol. 103, no. January, pp. 291–307, 2019, doi: 10.1016/j.rser.2018.12.048.

[81] "Resistivity-Conductivity Formula." https://softschools.com/formulas/physics/resistivity_conductivity_formula/525/?msclkid=fefdf81ad04811ec89483d71d2551e83 (accessed May 10, 2022).

[82] X. Li *et al.*, "Functional Groups Determine Biochar Properties (pH and EC) as Studied by Two-Dimensional 13C NMR Correlation Spectroscopy." plosone, 2013. doi: https://doi.org/10.1371/journal.pone.0065949.

[83] R. S. Gabhi, D. W. Kirk, and C. Q. Jia, "Preliminary investigation of electrical conductivity of monolithic biochar," *Carbon N. Y.*, vol. 116, pp. 435–442, 2017, doi: 10.1016/j.carbon.2017.01.069.

[84] Y. Dang, D. Sun, T. L. Woodard, L. Y. Wang, K. P. Nevin, and D. E. Holmes, "Stimulation of the anaerobic digestion of the dry organic fraction of municipal solid waste (OFMSW) with carbon-based conductive materials," *Bioresour. Technol.*, vol. 238, pp. 30–38, 2017, doi: http://dx.doi.org/10.1016/j.biortech.2017.04.021.

[85] J. Y. Lee, S. H. Lee, and H. D. Park, "Enrichment of specific electro-active microorganisms and enhancement of methane production by adding granular activated carbon in anaerobic reactors," *Bioresour. Technol.*, vol. 205, pp. 205–212, 2016, doi: 10.1016/j.biortech.2016.01.054.

[86] T. G. Ambaye, M. Vaccari, E. D. van Hullebusch, A. Amrane, and S. Rtimi, "Mechanisms and adsorption capacities of biochar for the removal of organic and inorganic pollutants from industrial wastewater," *Int. J. Environ. Sci. Technol.*, 2020, doi: doi.org/10.1007/s13762-020-03060-w.

[87] L. Xiao, E. Lichtfouse, P. S. Kumar, Q. Wang, and F. Liu, "Biochar promotes methane production during anaerobic digestion of organic waste," *Environmental Chemistry Letters*, vol. 19, no. 5. pp. 3557–3564, 2021. doi: 10.1007/s10311-021-01251-6.

Appendices

Appendix A Project Description

University of South-Eastern Norway
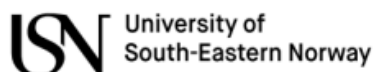
Faculty of Technology, Natural Sciences and Maritime Sciences, Campus Porsgrunn

FMH606 Master's Thesis

Title: Analysing biocarbon from pyrolysis in anaerobic digestion

USN supervisor: Wenche Bergland and Nabin Aryal

External partner: Pål Jahre Nilsen and Gudny Øyre Flatabø in Scanship AS

Task background:

In a circular economy waste streams must be handled to utilize their material and energy potentials. Organic waste streams can be treated in different ways depending on their contents. Easily degradable organic waste can be anaerobic digested to get the biomethane potential. Organic waste rich in lignocellulose can be pyrolysed to produce biochar, bio oil and syngas. Combining anaerobic digestion (AD) and pyrolysis is an active research field to improve handling and utilization of organic waste streams. It is economically beneficial to reduce the amount of handling processes for one type of waste, and utilizing biochar, bio oil and syngas in AD can be an advantage. Biochar mechanisms in AD are not fully understood and this thesis is part of a project to analyse possible biochar advantages in full-scale AD reactors.

Task description:

• Literature review study.

• Testing biochar derived by pyrolysis process from Scanship AS and then compare with commercially available activated carbon to optimise AD process.

• Analysing biochar and activated carbon in BMP test

• Characterisation of biochar such as spatial surface evaluation of biochar produced at Scanship AS through Scanning Electronic Microscopy (SEM), biocompatibility test etc

• Applying SEM technique to evaluate the biofilm on biochar

• Data analysis and interpretation to understand the AD process.

Student: Reserved for EET student Nasim Mohajeri Nav
Is the task suitable for online students (not present at the campus)? No

Practical arrangements:
Laboratory work is mostly to be undertaken at USN campus Porsgrunn except when using SEM that is at USN campus Vestfold.

Supervision:
As a general rule, the student is entitled to 15-20 hours of supervision. This includes necessary time for the supervisor to prepare for supervision meetings (reading material to be discussed, etc).

Signatures:
Supervisor (date and signature): 01.02.22   *Wenche Bergland*

Student (write clearly in all capitalized letters): Nasim Mohajeri Nav
Student (date and signature): 27.01.2022, Nasim Mohajeri Nav

Appendix B Optimum Growth pH of Some Methane-forming Bacteria

Genus	pH
Methanosphaera	6.8
Methanothermus	6.5
Methanogenium	7
Methanolacinia	6.6-7.2
Methanomicrobium	6.1-6.9
Methanospirillium	7.0-7.5
Methanococcoides	7.0-7.5
Methanohalobium	6.5-7.5
Methanolobus	6.5-6.8
Methanothrix	7.1-7.8

Appendix C Average Total Produced Biogas in the First Batch and their error bars
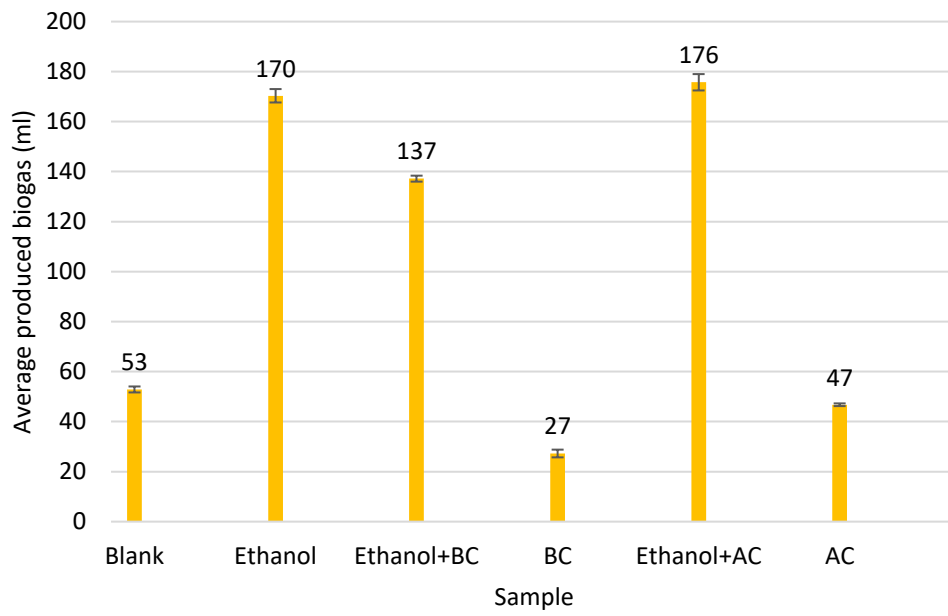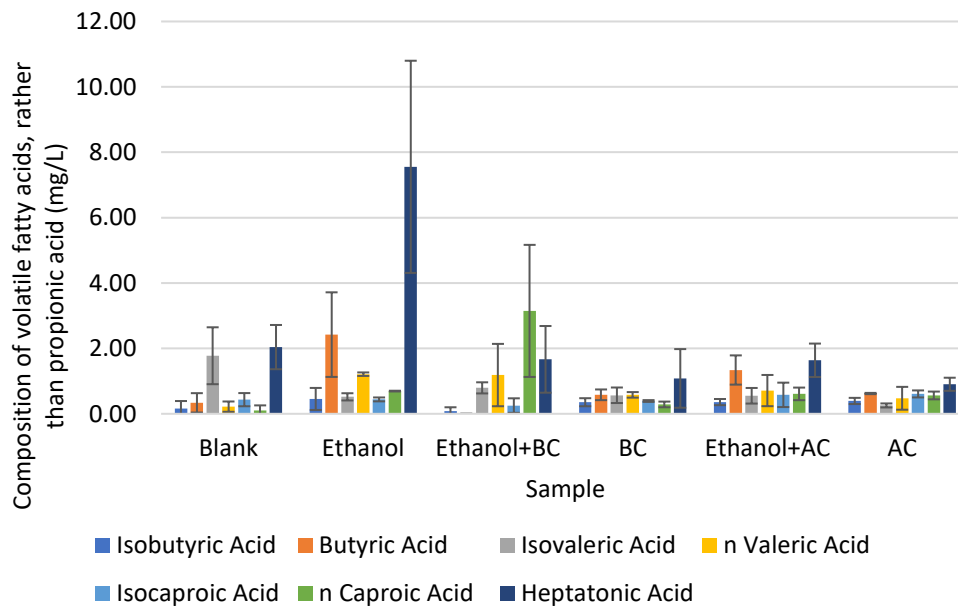
Appendix C Composition of volatile fatty acids at the end of the first batch
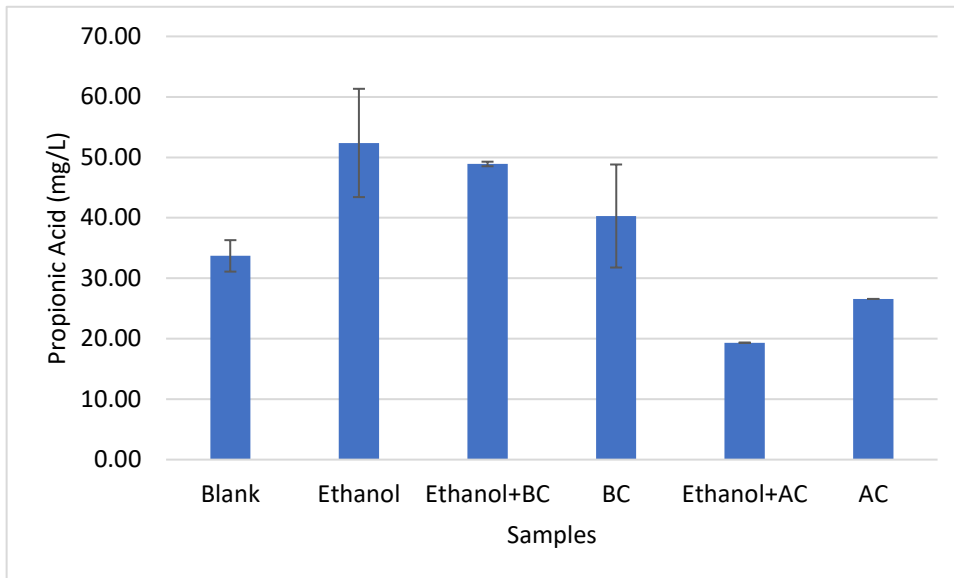
Propionic Acid:
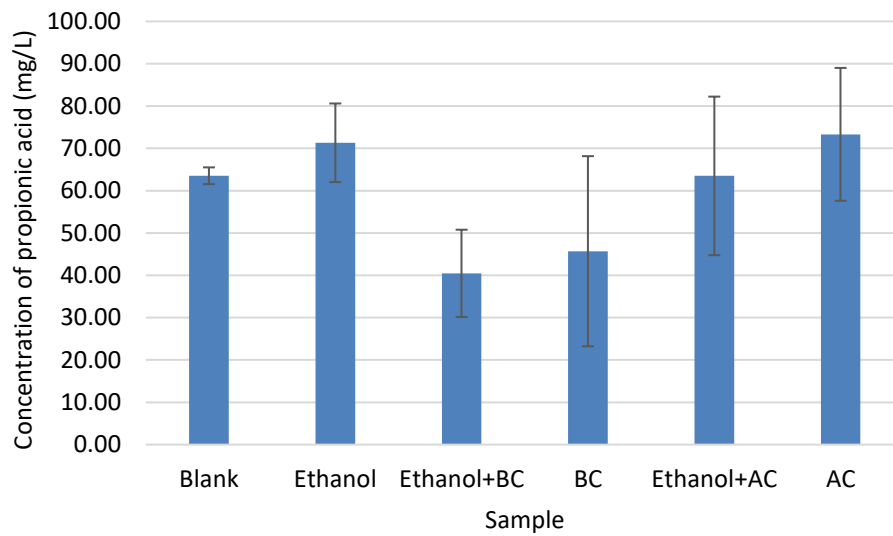
Other Acids:

Appendix D Composition of volatile fatty acids at the end of the second batch

Propionic Acid:

Other Acids: